THE UNIVERSITY OF CHICAGO

RNA N6-METHYLADENOSINE MODIFICATION MAINTAINS EPIDERMAL STEMNESS THROUGH PVT1-MYC INTERACTION

A DISSERTATION SUBMITTED TO

THE FACULTY OF THE DIVISION OF THE BIOLOGICAL SCIENCES

AND THE PRITZKER SCHOOL OF MEDICINE

IN CANDIDACY FOR THE DEGREE OF

DOCTOR OF PHILOSOPHY

COMMITTEE ON CANCER BIOLOGY

BY

JIMMY LEE

CHICAGO, ILLINOIS

MARCH 2022

TABLE OF CONTENTS

LIST OF FIGURES

ACKNOWLEDGEMENTS

This has been a long journey for me, and I would not have made it without the help of numerous people along the way.

First, I would like to thank all the lab members from Wu lab. Cynthia is a senior graduate student in the Cancer Biology Committee, and was able to give me numerous advices on both lab work and navigating the program. She was always very eager to help and answer my questions. Jiping was the post-doc in the lab when I first joined. He was a treasure trove of knowledge and can always give me a thorough explanation on any biology questions I throw at him. In addition, he was also highly experienced in performing complex experiments such as skin grafting. He taught me how to perform the grafting experiment, which became an important part of my thesis research. Even as he left the lab, he continued to give me career advices and suggestions. Xuewen was the lab manager when I joined, he showed me around the lab and welcomed me warmly, making me feel like a family.

Later on, Yuchen and Zhigang came to the lab as visiting scholars. This was when I started to delve deeper on my thesis work, and felt overwhelmed by the large amount of assays to optimize and perform. Yuchen helped me with many cell assays, which helped greatly alleviated my load. Zhigang, while not directly involved in my project, gave me many insights from a different prospective as he was specialized in organic chemistry. James was a new post-doc and we had many collaborated works. We also had constant brain storming on ideas on

new biomaterials, which was very inspiring. Lifeng, Sarah and Alex also joined the lab as graduate students and I was able to learn a lot from them when we discussed our projects and share feedbacks. Jing as the new lab manager helped me greatly making all the orders in a timely manner. Finally, Suman was the new post-doc to come after Jiping left. Like Jiping, she had a lot of experience in basic cell and molecular biology assays and I could always learn something new from talking with her.

I would also like to thank Bryan from the He lab. I had very limited experiences working on RNA before I began my thesis work. Bryan offered me tremendous help, giving me advice on how to design assays, analyze data, and shared his protocols with me, saving me a lot of time and effort in my research. In addition, he also helped me with the experiments on m^6A sequencing as well as mass spectrometry. The thesis could not have been completed without his help.

Next, I would like to acknowledge Chang and Catherine from the Becker lab next to us. Chang was also a senior graduate student in the Cancer Biology Committee and offered me many good advices on my research and let me use their flow cytometry machine. Catherine allowed me to use their cryostat in the lab at a critical moment, as all the core facility were locked down at that time due to Covid and I needed to make some sections to acquire data requested by reviewers. With their help I was able to complete my thesis work with minimal delay.

I want to next thank my thesis committee members. Dr. Yu-Ying He was the committee chair and always gave me encouragements and steered me on the right direction. Dr. Kay Macleod, who gave me many critical comments during our committee meetings and allowed me to reinforce my proposal and experimental designs. In addition, I am very grateful for her for allowing me to join the Committee of Cancer Biology, when the Committee of Molecular Medicine and Pathogenesis, where I originally applied for, was dissolved. Dr. Chuan He, who was the leading expect in RNA m^6A modification, not only provided me his lab resources to work on this topic, but also gave numerous suggestions on how to improve my work. I understand that he is a very person, and I really appreciate him agreeing to join my thesis committee and find time to participate in the meetings.

Last but not least, my thesis committee member and thesis advisor, Dr. Xiaoyang Wu. When I first heard about his work during one of the faculty talks, I was immediately captivated by the originality of his ideas in solving clinical problems with basic cellular and molecular tools. I proposed a high-risk project when I started in the lab, and he was supportive of my work. Even though it did not work out in the end, I was very grateful that he gave me the chance to shoot for something big. Additionally, he also provided me with an idea for a “back-up” project, which eventually become this thesis research. Dr. Wu has a very good understanding of human diseases and could always come up with interesting ways to tackle them. He is never afraid of taking up a risker project, yet he does not get over drown into any of these projects

and can pull out from them when the data does not support the hypothesis. I always feel I have so much to learn from him, not only on designing experiments to prove hypotheses, but also on how to see the big picture and move forward, which I feel is the hardest skill as a primary investigator. In addition, Dr. Wu is a wonderful person to work with, always gentle and to the point, and never using harsh languages or hyperboles. He works diligently himself, but allows us to work on our own time scale. Dr. Wu showed me how someone could manage a productive lab without being a pushing mentor.

Next, I want to acknowledge my friends along this journey. Lucy Yang, my classmate in medical school and long-time friend in science. It seemed like we were the only persons in the class who were serious about basic science, and it was great to have someone like-minded to traverse this windy pass. Seenu, who welcomed me when I first visited the University of Chicago, and continued to support and encourage me throughout my time here, his warmth made this cold and distant land feel like home. Alicia, who introduced me to the graduate program at the University of Chicago and let me learn a lot about the scientific developments going on here.

I want to thank my former mentors. Dr. Ching-Feng Cheng, who let me work in his lab as a summer student when I was in medical school, and inspired me to become a physician scientist like him. Dr. Oscar Lee, who started my interest in stem cell science, and showed me how a small lab and become competitive by focusing on things that mattered. Dr. Ming-Yuan

Lee, who trained me in as a resident in anatomical pathology and encourage me to pursue a PhD degree. Dr. Lynn Wang, who let me join her lab when I first came to the University of Chicago and continued to give me advices on how to navigate between being a pathologist and a scientists.

Finally, I want to acknowledge my family members. My Dad inspired me to become a scientist early on in my life, and was always the scientist model for me. I have figured out long ago that I could never come close to his scientific achievements, but I am content with what discoveries I have and can make. Science is a process of assimilation of knowledge, and small discoveries, like little streams, can still converge into a river, even if they originate from different hills or mountains. My mother was always very caring and supportive of me. No matter what I did she will always be there for me. She also made aware of the career path of a clinician, which I originally thought would not suite me, but eventually turned out to be a good fit, and I am very glad I made the decision to enter medical school. I am also grateful to my brother, David, who always looked after me as we grew up, and served as a role model then and now. He is someone I will always respect and trust. My sister Sofia, who was very perceptive and thoughtful. I could discuss anything with her and get very useful feedback. My wife, Angie, who was always very understanding and considerate, and my daughter, Clio, who gave me the opportunity to pass on the love I received from my parents. I also want to thank my uncle, HM, who introduced me to the University of Chicago, which started this journey.

He also looked after me throughout my stay in Chicago and made sure I had everything I needed.

This dissertation is written in memorial of two special persons in my family. First is my grandfather, who passed away right before I was applying to a graduate program. He lived in a turbulent time that was full of challenges and uncertainty, but through his strong will and hard work, he created a stable environment for the family and allowed us to pursuit our interests. He always showed interest in my progress during medical school, and I believe he would also have been pleased to hear about my thesis work. The second is my cousin, Alex, who passed away a few months before my defense. We played together as kids, and continued to stay in touch throughout the years. He came to my wedding in Taiwan, and also visited me frequently when I was in Chicago. I am certain that he would have come here for my defense and celebrate with me afterwards.

CHAPTER I

INTRODUCTION

The structure and development of the skin

The skin lies at the surface of the human body, offering a physical barrier against environmental hazards from without, while also preventing excessive water loss from within[1,2]. The structure of the skin has been well studied in the past, documented as early as the third century BCE[3], but a more refined appreciation of its structure wasn't possible until the development of light microscopy, and centuries later, electron microscopy. In general, the mammalian skin can be divided broadly into the epidermis and dermis. The dermis is composed mainly of connective tissue and provides a foundation for the epidermis. It also contains blood vessels and lymphatics that supply the epidermis, as well as hair follicles, sweat glands, and nerve fibers.

The epidermis is above the dermis and constitutes the main protective barrier of the skin. It can be further divided into four layers, from superficial to deep: the corneal layer, the granular layer, the spinous layer, and the basal layer. The basal layer lies at the base of the epidermis, and is composed of basal cells anchored to the basement membrane, which is the interphase between epidermis and dermis. The basal cells constantly proliferate, giving rise to differentiated keratinocytes, which migrate towards the upper layers[4-8]. As keratinocytes migrate and differentiate, they acquire distinct morphological features seen in each layer: the

intercellular spinous ridges in the spinous layer, which is in fact a fixation artifact created by intercellular tight junctions, the hyaline granules in the granular layer, and the flat, anuclear cells in the corneal layer (**Figure 1.1**). In addition to the difference in cellular morphology, the undifferentiated basal cells and the differentiated suprabasal cells can also be distinguished by different sets of keratin proteins expressed in the cells, with the former expressing keratin 5(Krt5) and keratin 14(Krt14) and the latter expressing keratin 1(Krt1) and keratin 10 (Krt10). The keratinocytes are the main component of the epidermis and are responsible for creating the physical barrier. Other cells types are also present in the epidermis, including melanocytes, Langerhans cells, and Merkel cells. Melanocytes generate melanin pigments, which are taken up by the keratinocytes and provide protection against ultraviolet light damage while also giving the skin a darker appearance. Langerhans cells are specialized dendritic cells that provide a first line of immunological defense in the skin. Merkel cells contain mechanoreceptors and can transmit light touch sensations.

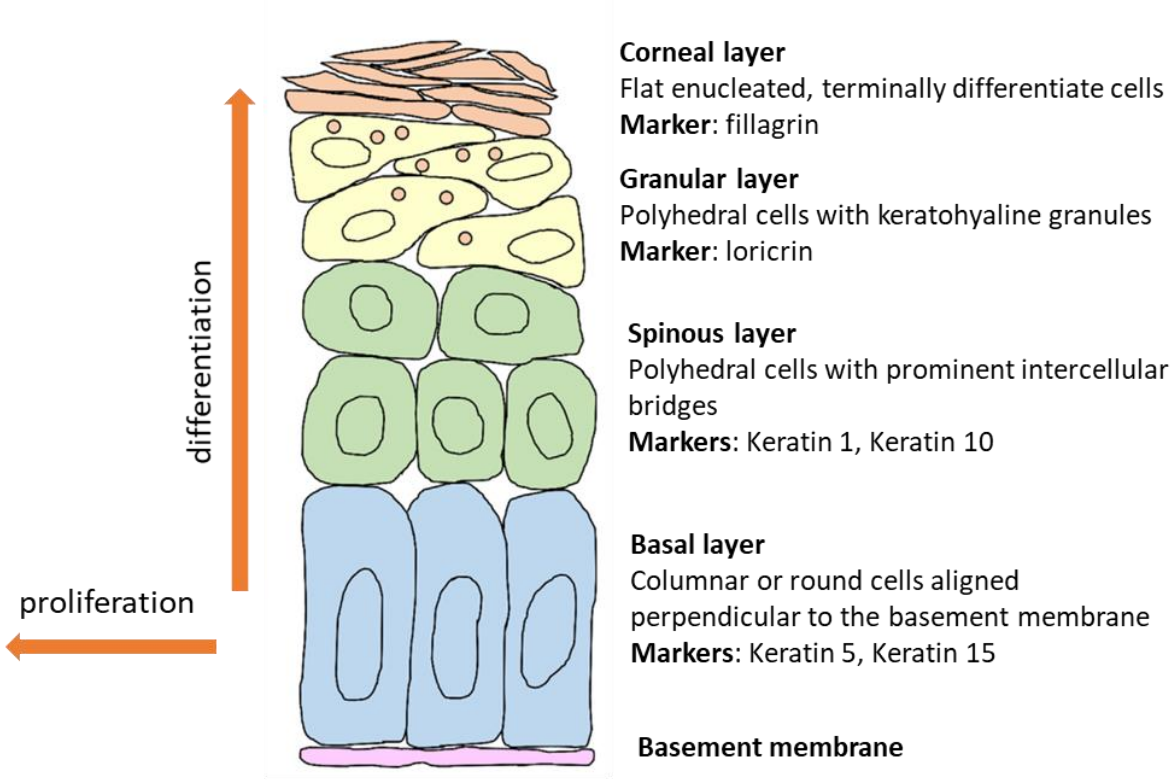

Figure 1.1: Epidermis layers and skin differentiation. The cross section of the epidermis and the basement membrane underneath is depicted. Basal keratinocytes are attached to the basement membrane and are the only proliferative cells in normal skin epidermis. When basal cells proliferate, they can replenish the stem cell pool, or differentiate and migrate upwards as depicted on the left. When basal cells are committed to differentiation, they move away from the basement membrane and generate three layers of differentiated cells: the spinous layer, granular layer and corneal layer. Key morphological features and protein markers of each layer are shown in the right.

Genetic regulators of skin homeostasis

The skin, as superficial and plain as it may seem, conceals great depth and complexity in its intricate regulatory mechanisms. Indeed, the skin is a tightly regulated organ with constant turnover, which is essential for maintaining its protective function[1]. Loss of homeostasis can lead to various skin diseases, including skin squamous cell carcinoma[9]. Epidermal homeostasis consists of a balancing act between proliferation and differentiation of the epidermal stem cells.

While the precise regulatory mechanism of skin homeostasis remains elusive[10], a few central players have been identified. One of the more well-established drivers of epidermal basal cell stemness is the transcription factor p63[11], which can maintain proliferating basal keratinocytes by suppressing cell cycle inhibitors, including p21, Ink4a, and Arf, while inducing the expression of cell cycle genes[12]. Loss of *P63* leads to severe defects in skin epithelium, resulting in loss of barrier function and prenatal death in mice[13]. In humans, mutations in the *P63* gene also leads to numerous skin defects, such as ectodermal dysplasia[14].

Another critical regulator of epidermal stem cells is *MYC*. *MYC* is perhaps most well-known as one of the four "Yamanaka factors" capable of reprogramming differentiated cells, indicating its dominant role in driving stem cell fate[15,16]. Not surprisingly, *MYC* is also critically involved in epidermal homeostasis[17-20]. MYC is highly expressed in the basal cells and down-regulated in the differentiated cells[21], and can maintain epidermal stemness via several pathways. For example, MYC can drive the expression of *NSUN2* (NOP2/Sun RNA Methyltransferase 2, also known as MISU) and induce cell proliferation[22]. MYC can also induce *SETD8* expression, which activates P63 and supports epidermal survival[23]. Conversely, *MYC* ablation leads to impaired epidermal homeostasis[20]. While there is strong evidence supporting MYC's being one of the master regulators in epidermal stem cells, it is likely the level of MYC is finely balanced to fit this role, and how this is achieved remains unsolved[21].

The role of lncRNA in skin homeostasis

Long non-coding RNAs (lncRNAs) are RNAs that are longer than 200 nucleotides and not translated into functional protein. It is estimated that the human genome contains 10,000 to 100,000 lncRNAs. The majority of the lncRNAs have no known function and are considered translational by-products. However, a growing number of lncRNAs have been found to play important roles in cell regulation, which can be achieved through their interaction with DNA, RNA or protein[24].

Various lncRNAs have been implicated in regulating skin homeostasis[25,26]. ANCR (anti-differentiation ncRNA, also known as DANCR) and TINCR (terminally-induced ncRNA) are among the earliest lncRNAs reported to regulate tissue differentiation. ANCR can maintain epidermal stem cell state by suppressing differentiation genes[27], whereas TINCR supports epidermal differentiation by forming a complex with STAU1 protein that stabilizes differentiation mRNAs[28]. More recently, many additional lncRNAs have been reported to contribute to skin homeostasis, including SMRT2 (squamous cell carcinoma misregulated transcript-2)[29], BLNCR (beta1-adjacent long non-coding RNA)[30], LINC000941[31], uc.291[13] and PRANCR (progenitor renewal associated non-coding RNA)[32]. SMRT-2 and uc.291 promote epidermal differentiation. Conversely, BLNCR, LINC000941, and PRANCR maintain epidermal stem cell self-renewal and survival. Most of these lncRNAs were discovered through sequencing studies and screening assays, and it is likely that there are still many undiscovered

lncRNAs that may have a role in skin homeostasis.

Chemical modifications on RNA

As with DNA and protein, RNA can also be chemically modified to fine tune its function[33,34]. The external modifications at the 5' cap and 3' poly-A tail on mRNAs are among the first discovered RNA modifications and have been found to play important roles in transcript transportation, splicing, and translation. With the advent of analytical chemistry and high-throughput sequencing methods, many additional mRNA modifications have been uncovered in the past decade.

N^6-methyladenosine (m^6A) is the most common internal mRNA modification and occurs in poly-adenylated RNAs, including mRNA and lncRNA[35]. The regulatory mechanism of m^6A modification, as well as its role in both stem cell development and cancer pathogenesis, has been intensively studied and will be the focus of the next two subchapters. Methylation can also occur at the N^1 position of the mRNA (m^1A). The N^1 position is located at the Watson-Crick interface and m^1A generates a positive charge, which can affect RNA-protein interaction or RNA secondary structure[36,37]. N^1-methyladenosines occurs almost exclusively at the translation start site and m^1A can facilitate transcript translation. Finally, the N^6, 2'-O-dimethyladenosine (m^6Am) is another adenosine methylation that occurs at the translation start site[38,39]. The methyltransferase PCIF1 has recently been identified to generate m^6Am and can increase the stability of the modified transcript[40].

As with the cytosine in DNA, the cytosine in RNA can also be methylated (m^5C), though the modification is less abundant compared to m^6A[41-43]. The m^5C modification is generated by the methyltransferase NSUN family (primarily NUSN2) as well as DNMT2, and can occur on a wide range of RNA species, including rRNA, tRNA, mRNA, lncRNA, and mitochondrial RNA[44-46]. The function of m5C is also diverse and depends on the modified RNA. For example, it can facilitate ribosome assembly in rRNA or increase nuclear export in mRNA. And as with methylcystosine in DNA, the RNA methylcytosine can be further oxidized by the TET2 (ten eleven translocation 2) protein to generate 5-hydroxymethylcytosine (hm^5C)[47]. Current evidence suggests that hm5C occurs mostly on tRNA and its main function is to facilitate tRNA assembly[48].

Mechanisms of RNA m^6A modification

RNA m6A modification was first reported in 1974 as the most prevalent form of RNA methylation[41]. The majority of m^6A modifications are distributed near the stop codons and 3' untranslated region (3'UTR) on the transcripts, and the modification is installed on a specific sequence motif RRACH (R=A/G, H=A/C/U)[49-51]. m^6A is generated by a writer protein complex composed of multiple protein subunits, though at its core is the heteroduplex METTL3 (methyltransferase-like 3) and METTL14 (methyltransferase-like 14)[52,53]. METTL3 provides the catalytic function, whereas METTL14 is essential for RNA binding.

The transcript specificity of m^6A modification is regulated via several elements that can direct METTL3 or METTL14 to certain transcripts[54,55]. For example, after ultraviolet radiation, METTL3/METTL14 can localize to the site with DNA damage and increase m^6A abundance[56]. The methyltransferase complex can also interact with transcription factors of the SMAD family to facilitate m^6A modification on the SMAD-driven transcripts[57]. Finally, modified histone can also play a role in coordinating m^6A modification, as the histone H3 lysine trimethylation (H3K36me3) has been shown to recruit METTL14[58].

In addition to the METTL3/METTL14 complex, two novel m^6A methyltransferases have been recently reported: METTL16 (methyltransferase-like 16) and ZCCHC4 (Zinc Finger CCHC-Type Containing 4), though with very different substrates. METTL16 generates m6A modification on U6 small nuclear RNA (snRNA) as well as the MAT2A mRNA[59-61], whereas ZCCHC4 targets 28s rRNA[62,63].

RNA m^6A modification can be removed by two demethylases, FTO (fat mass and obesity-associated) and ALKBH5 (AlkB homolog 5). FTO not only removes m^6A modifications from mRNA, but also demethylates m^1A from tRNA and m^6Am from snRNA and mRNA[64,65]. In contrast, currently ALKBH5 has only been reported to demethylate m^6A[66]. FTO and ALKBH5 each have distinct tissue distribution patterns, with FTO being more concentrated in the central nervous system[67] and ALKBH5 in the testis[66], which may account for their different biological roles.

In addition to the "writer" and "eraser" proteins, which add and remove m^6A, there are also "reader" proteins that interact with m^6A and dictate the functional consequences of the modified RNA. The m^6A reader is a rapidly expanding class of proteins with a wide range of functions. The YTH (YT521-B homology) family proteins YTHDF1-3 (YTH domain family 1-3) and YTHDC1-2 (YTH domain containing 1-2) are the among the earliest m^6A readers identified. YTHDF2 facilitates the degradation of the m^6A-modified transcripts[68,69], whereas YTHDF1 and YTHDF3 support the translation of the transcript[70,71]. YTHDC1 regulates splicing[72,73], whereas YTHDC2 increases transcript stability[74,75]. Another type of reader protein can interact with RNA only after it has been modified with m^6A, which changes its conformation and allows RNA-protein interaction, a mechanism referred to as the "m^6A-switch". This was first reported in HNRNPs (heterogeneous nuclear ribonucleoproteins) such as HNRNPC[76]. Other reported m^6A reader proteins include IGF2BP1-3 (insulin-like growth factor 2 mRNA-binding protein 1-3)[77,78], FMRP (fragile X mental retardation protein)[79] and Prrc2a (proline rich coiled-coil 2A)[80]. As the readers are the ultimate determinant of m^6A function, they are represented by a diverse class of proteins with context dependent roles, and the list is likely to continue to expand rapidly in the coming decade.

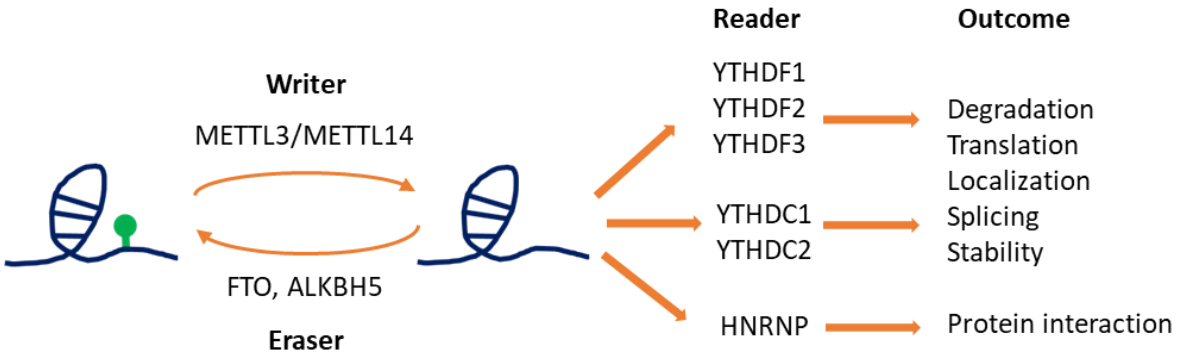

Figure 1.2: Various proteins regulate RNA m6A modification. METTL3 and METTL14 forms the core of the writer protein and transfer methyl groups to specific sites on polyadenylated RNAs. Eraser proteins, including FTO and ALKBH5, can remove the methyl group. Modified RNAs can have a broad range of outcomes depending on the different reader proteins.

RNA m^{6}A modification in development and disease

The importance of RNA m^{6}A modification in regulating the developmental process is best demonstrated by the detrimental effect of depleting *METTL3* or its homologs in various model organisms. In yeasts, knocking out *IME4*, the *METTL3* homolog, leads to impaired meiosis[81], whereas in drosophila, *IME4* knockout causes developmental arrest[82]. Knockout of either *METTL3* or *METTL14* is embryonically lethal in mice, and in both human and mouse embryonic stem cells, *METTL3* knockout drives the stem cells into a differentiation fate[83,84]. While m^{6}A modification can regulate gene expression through a wide range of methods, its essential function in controlling stem cell development may lie in its function to create groups of transcripts that can be coordinated to facilitate cell fate transition[34,85]. Recent studies also shed light on the regulatory role of m^{6}A in different tissues. For example, it has been found to

be crucial for spermatogenesis in the testis[86], neurogenesis in the brain[87-89], maintaining β-cell function in the pancreas[90], immune cell regulation[91,92], and cardiac homeostasis[93].

Conversely, dysregulation of the m^{6}A machinery has been linked to a wide range of human pathologies, such as type 2 diabetes[94], cardiovascular diseases[95], chronic obstructive pulmonary disease[96], Alzheimer's disease[97], and viral infection[98]. In addition, a broad range of cancers have also been linked to m^{6}A dysregulation. These include acute myeloid leukemia (AML)[99-101], glioblastoma (GBM)[102-104], lung cancer[105,106], breast cancer[107,108], and hepatic cell carcinoma[109,110], with many others still under evaluation[111,112]. Interestingly, m^{6}A modification could act as both a driver for malignancy and also a tumor suppressor depending on the context. For example, in AML cells, overexpression of *METTL14* leads to increased m^{6}A modifications on MYC and MYB transcripts. These oncogenic transcripts are stabilized by the modification and in turn drive AML progression[100]. In contrast, glioblastoma stem cells depend on a low level of m^{6}A to maintain growth and self-renewal[104]. This observation attests to the context-dependent nature of m^{6}A modification, and extra care should be taken to untangle its regulatory role in a complex system.

CHAPTER II

RNA N^6-METHYLADENOSINE MODIFICATION REGULATES EPIDERMAL STEMNESS

INTRODUCTION

The skin acts as our first line of defense against various environmental hazards, such as microorganisms, chemical toxins, extreme temperature, and ultraviolet radiation. In addition, its role in preventing water loss is also vital to our body function. While static in appearance, the skin is one of the most dynamic organs of the body, as the old skin at the surface is shed off daily and replaced by newly differentiated skin cells from the lower layers. This constant turnover of skin tissue is achieved through a sophisticated balance between epidermal stem cell proliferation and differentiation[1,2]. While the genetic regulation of skin homeostasis has been the focus of skin research over several decades, recent findings are beginning to shed light on the potential role of epigenetic regulatory mechanisms that may fine-tune the transition between different epidermal cell fates[113-115].

The recent characterization of RNA N^6-methyladenosine (m^6A) modification has opened up a new chapter in epigenetic regulation. RNA with m^6A modification can lead to changes in stability, splicing, localization and translation[34,85]. It has been found that embryonic stem cells can rapidly respond to external cues and commit to differentiation through m^6A-mediated decay of pro-pluripotency transcripts[84]. RNA m^6A modification has also been found to be

essential during the development of immune[92] and neuronal systems[87], and dysregulation of m^{6}A modification protein is reported in various cancers[112]. While RNA m^{6}A modification has not yet been studied in skin development, our preliminary analysis showed that m^{6}A writers, including METTL3 and METTL14, have decreased expression level in differentiated skin. We thus hypothesized that RNA m^{6}A modification may play an important role in regulating epidermal homeostasis.

Using a mouse genetics approach, we found that conditional ablation of *Mettl14* in the skin epidermis resulted in impaired skin development, including fewer basal cells and aberrant differentiation. By isolating and culturing the Mettl14-depleted epidermal progenitor cells and utilizing a wide range of classical stem cell assays, we were able to demonstrate that the skin phenotype was due to an imbalance in the stem cell program, shifting the cells from proliferation to differentiation. Finally, to further characterize the RNA methylome that regulates epidermal proliferation and differentiation, we performed RNA m^{6}A-sequencing on epidermal progenitor cells before and after induced differentiation and found that RNA processing and metabolism pathways may be regulated by m^{6}A methylation. In addition, we also noticed several long non-coding RNAs (lncRNAs) showing significant changes in methylation level after differentiation. Our study shows that RNA m^{6}A modification plays an essential role in maintaining epidermal stemness, which may be achieved through methylation of lncRNAs.

MATERIALS AND METHODS

Antibodies and chemical reagents

Guinea pig Krt5, rabbit Krt10, and Loricrin antibodies were generous gifts from Dr. Elaine Fuchs at Rockefeller University. Rabbit Krt 14 and Krt 10 antibodies were obtained from Covance (Princeton, NJ). Rat monoclonal b4-integrin (CD104) was obtained from BD Pharmingen (Franklin lakes, NJ). P63 antibody was obtained from Genetex (Irvine, CA). METTL14 antibody was obtained from Sigma (St Louis, MO). MYC, GAPDH, and α-tubulin antibodies were obtained from ProteinTech (Rosemont, IL). HA-conjugated beads were obtained from Sigma (St. Louis, MO). Rabbit polyclonal antibodies against Ki67 were obtained from Santa Cruz Biotechnology, Inc. (Santa Cruz, CA). Other chemicals or reagents were obtained from Sigma, unless otherwise indicated.

Generation of *Mettl14* cKO mice

The *Mettl14* conditionally targeted strain (*Mettl14*$^{flox/flox}$) was kindly provided by Dr. Chuan He (University of Chicago). *Mettl14* conditional knockout (cKO) animals were generated by breeding the strain with *K14-Cre* or *K14-CreERT2*. To avoid a potential maternal effect, we used male mice with *K14-Cre* or *CreERT2* transgene for breeding. Genotyping was conducted by PCR of tail skin DNAs. All mice used in this study were bred and maintained at the animal resource center (ARC) of the University of Chicago in accordance with institutional

guidelines.

Quantification of RNA m6A modification levels via mass spectrometry

Total RNA was subjected to two rounds of poly(A) selection with the Dynabeads mRNA purification kit (Invitrogen). 25 ng of the purified mRNA was digested by nuclease P1 (1 U) in 20 µl of buffer containing 20 mM NH4OAc pH 5.5 at 42°C for 2 h, followed by the addition of FastAP buffer (2.3 µl, Thermo Scientific) and alkaline phosphatase (1 U) and incubation at 37°C for 4 h. The sample was then filtered (0.22 lm pore size, 4 mm diameter, Millipore), and 5 µl of the solution was injected into the LC-MS/MS (liquid chromatography-mass spectrometry/mass spectrometry). The nucleosides were separated by reverse-phase ultra-performance liquid chromatography on a C18 column (Agilent) with online mass spectrometry detection using a Sciex 6500+ triple-quadrupole LC mass spectrometer in positive electrospray ionization mode. The nucleosides were quantified by using the nucleoside-to-base ion mass transitions of 282–150 (m6A) and 268–136 (A). Quantification was carried out by comparison with a standard curve obtained from pure nucleoside standards run with the same batch of samples. The ratio of m^6A to A was calculated based on the calibrated concentrations.

Histology and immunostaining

For FFPE (formalin-fixed paraffin-embedded) tissue, skin samples were fixed in 10%

formalin for 24 hours, then dehydrated via xylene exchange overnight and embedded in paraffin. 0.5 μm sections were made and stained with HE (hematoxylin and eosin). For immunohistochemistry staining (IHC), sections were stained on a Leica Bond RX automatic stainer. Epitope retrieval solution II (Leica Biosystems, AR9640) was used for 20 minutes\ heat-induced antigen retrieval (HIAR). Antibodies were applied on tissue sections for 60 minutes of incubation and the antigen-antibody binding was detected with Bond polymer refine detection (polymer HRP, Leica Biosystems, DS9800). For quantification, slides were inspected under the microscope at high power (400x magnification) and epidermal cells were counted manually by a trained pathologist.

For frozen sections, skin samples were embedded in Tissue-Tek OCT compound (Sakura) and 0.7 μm sections made on a cryostat. The sections were fixed in 10% formalin and stained with HE. For immunofluorescence staining (IF), sections were fixed in 4% paraformaldehyde, permeabilized in 0.1% Triton X100 and blocked in blocking solution (2.5% normal goat serum, 2.5% normal donkey serum, 2% gelatin, 0.1% Triton X100 and 1% bovine serum albumin in PBS).

Skin wound healing assay

For skin wound healing assays, same sex littermates of ~12-week old mice were anesthetized and two full-thickness excisional wounds were made on both sides of the dorsal

midline following a previously described protocol[116]. Mice were housed separately and no self-induced trauma was observed in control or cKO mice. Tissue was collected 2–6 days after wounding and wound re-epithelialization was evaluated by histological analyses. Hyperproliferative epidermis was identified by HE staining and the length that extended into the wounds was measured and quantified.

Cell culture

Primary mouse keratinocytes were isolated from the epidermis of newborn mice using trypsin after prior separation of the epidermis from the dermis by an overnight dispase treatment. Keratinocytes were plated on mitomycin C–treated 3T3 fibroblast feeder cells until passage three. Cells were cultured in E-media supplemented with 15% serum with a final concentration of 0.05 mM Ca^{2+}.

Protein biochemical analysis

Western blot was performed as described previously[117]. Cell lysates were prepared with RIPA (radioimmunoprecipiation assay) buffer (50 mM HEPES pH 7.4, 150 mM NaCl, 10% Glycerol, 1.5 mM MgCl2, 1 mM EGTA, 1% Triton X-100, 1% Sodium Deoxycholate, 0.1% SDS) containing protease inhibitors and phosphatase inhibitors. Equal amounts of the cell lysates were separated using SDS-polyacrylamide gel electrophoresis (PAGE) and

electroblotted onto a nitrocellulose (NC) membrane. The immunoblot was incubated with Odyssey blocking buffer (Li-Cor) at room temperature for 1 hour, followed by an overnight incubation with the primary antibody. Blots were washed three times with Tween 20/Tris-buffered saline (TBST) and incubated with a 1:10,000 dilution of secondary antibody for 1 hour at room temperature. Blots were washed three times with TBST. Visualization and quantification were carried out with a LI-COR Odyssey scanner and software (LI-COR Biosciences, Nebraska, USA).

Analysis of m^{6}A-sequencing

Total RNA was isolated from primary mouse keratinocyte with or without calcium shift-induced differentiation. Polyadenylated RNA was further enriched from total RNA using a Dynabeads mRNA purification kit (Invitrogen). RNA was fragmented using a Bioruptor ultrasonicator (Diagenode) with 30 second on/off for 30 cycles. m^{6}A-immunoprecipitation was performed using a Epimark N6-methyladenosine enrichment kit (New England Biolabs) and library preparation was performed using an Illumina TruSeq Stranded mRNA Sample Prep Kit according to previously published protocols[118]. Sequencing was carried out at the University of Chicago Genomics Facility on an Illumina HiSeq4000 machine in single-read mode with 50 base pairs per read. m^{6}A-seq data were analyzed according to the protocol previously described[119]. Briefly, HISAT2 (version 2.1.0)[120] was used to align the sequence reads to

reference genome and transcriptome (mm10). Then, the exomePeak R/Bioconductor package (version 3.7) was used to find m^{6}A peaks and the QNB package (version 1.1.11)[121] was used to identify differentially methylated regions. Significant peaks with false discovery rate less than 0.05 were annotated to the RefSeq database (mm10). Differential gene expression was calculated using DESeq2 (version 1.18.1) using the sequencing reads from input samples[122]. Gene ontology (GO) analysis on the differentially methylated genes was performed using the Cytoscape app with BINGO plugin[123]. Gene Set Enrichment Analysis was performed using GSEA software created by Broad Institute[124,125].

Statistical analysis

Statistical analysis was performed using Excel, OriginPro, GraphpadPrism or SciDAVis software. Box plots were used to describe the entire population without assumptions about the statistical distribution. A Student's t-test was used to assess the statistical significance (P value) of the difference for the experiments.

RESULTS

***Mettl14* depletion in skin leads to defects in skin homeostasis and regeneration**

To investigate our hypothesis that RNA m^{6}A-modification contributes to epidermal homeostasis, we first tested whether loss of m^{6}A-modification can lead to phenotypic changes in skin. *Mettl14* knockout is embryonically lethal in mice[126]. We thus developed a skin

conditional knockout (cKO) model of *Mettl14*. A targeting cassette with two loxP sites was engineered into the *Mettl14* locus in mouse chromosome 3 by homologous recombination[87]. To conditionally delete *Mettl14* in the skin epithelium, we bred *Mettl14*$^{fl/fl}$ mice with transgenic mice carrying *K14-Cre* recombinase, which can efficiently excise floxed genomic DNA by embryonic day E15.5[116,127](**Figure 2.1 A, B, C**). *Mettl14* cKO mice were born in the expected Mendelian ratio but exhibit significant perinatal lethality. *Mettl14* cKO animals are smaller and often have tighter, smoother, and shiny skin compared with their wild type (WT) littermates (**Figure 2.1 D**). Immunohistochemistry confirms loss of Mettl14 in skin epithelial cells in the cKO animals (**Figure 2.1 E**). In addition, mass spectrometry analysis showed a dramatic decrease in global mRNA m^{6}A modification in *Mettl14* cKO skin epidermis, consistent with the known role of Mettl14 as an indispensable m^{6}A writer protein (**Figure 2.1 F**).

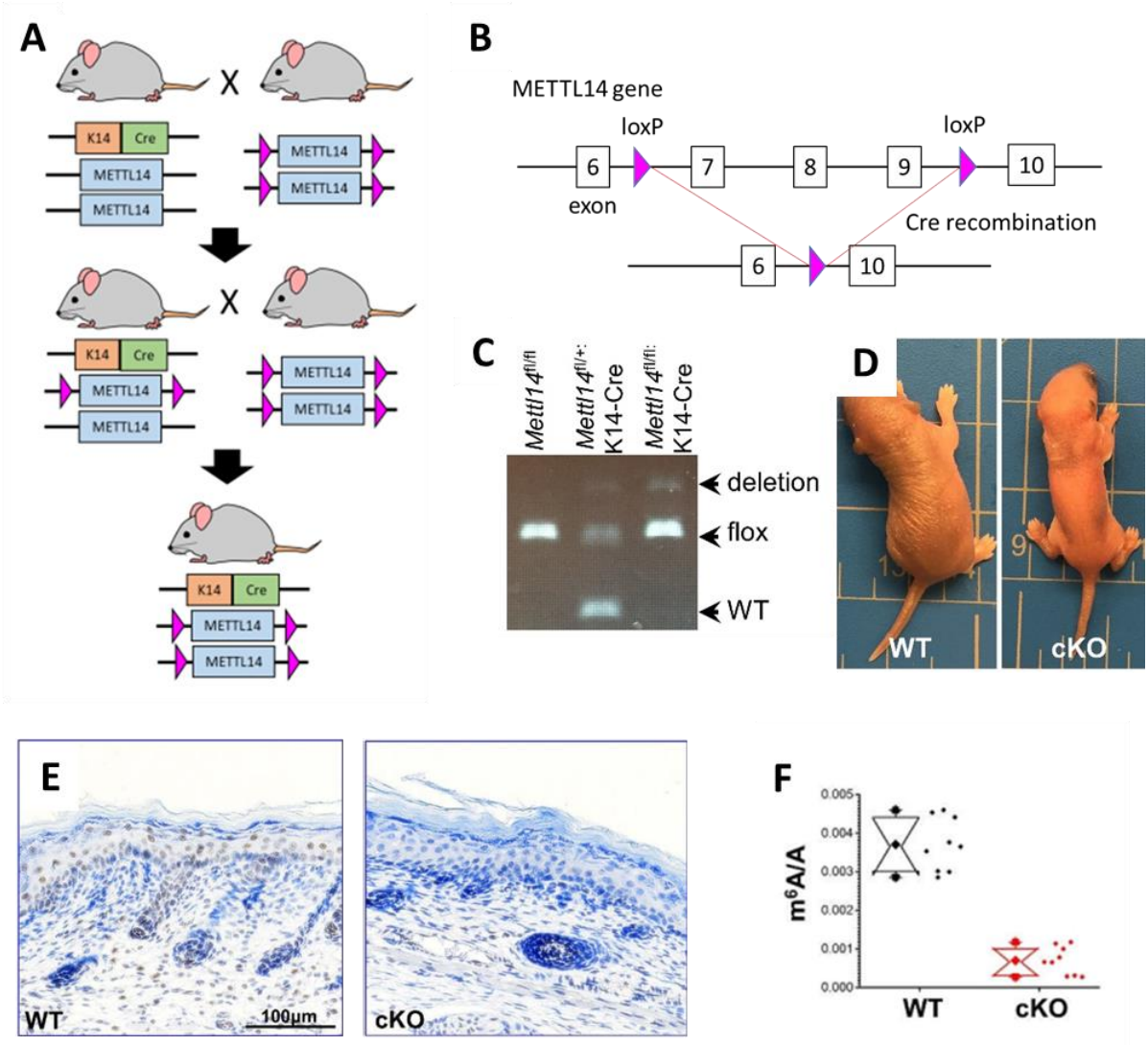

Figure 2.1: **Development of *Mettl14* cKO mice. A.** Schematic illustration of the breeding program for developing the *Mettl14* cKO mice. **B.** Schematic illustration of the Cre recombinase reaction that removes exon 7-9 from the METTL14 gene. **C.** Representative genotyping results for mice bearing *Mettl14*^{fl} and *K14-Cre* alleles. fl: floxed. **D.** *Mettl14* cKO pup (P3) with a WT littermate. Note the small size and shiny skin appearance of the cKO mice. **E.** Immunohistochemistry confirms loss of Mettl14 expression in skin in cKO animals. **F.** Level of total RNA m6A modification in WT and *Mettl14* cKO skin were determined by mass spectrometry and shown in a box and whisker plot. The plot indicates the mean (solid diamond within the box), 25th percentile (bottom line of the box), median (middle line of the box), 75th percentile (top line of the box), 5th and 95th percentile (whiskers), 1st and 99th percentile (solid triangles) and minimum and maximum measurements (solid squares). n=9 (biological repeats), $P<0.01$ (Student's t-test).

To understand the role of Mettl14 in skin development, we analyzed WT and *Mett14* cKO skin from newborn pups. Skin histology shows that the epidermis of the cKO mouse is noticeably thicker with a decreased number of hair follicles (**Figure 2.2 A**). Transcription factor p63 is a master regulator controlling epidermal morphogenesis and stemness[12,13]. Immunofluorescence staining demonstrates a significantly reduced number of p63-positive basal cells in cKO skin (**Figure 2.2 B, C**). Along with decreased and disoriented basal progenitor cells, *Mettl14* cKO skin epidermis has an expanded spinous layer as determined by staining with the early differentiation marker Keratin 10 (**Figure 2.2 D, E**).

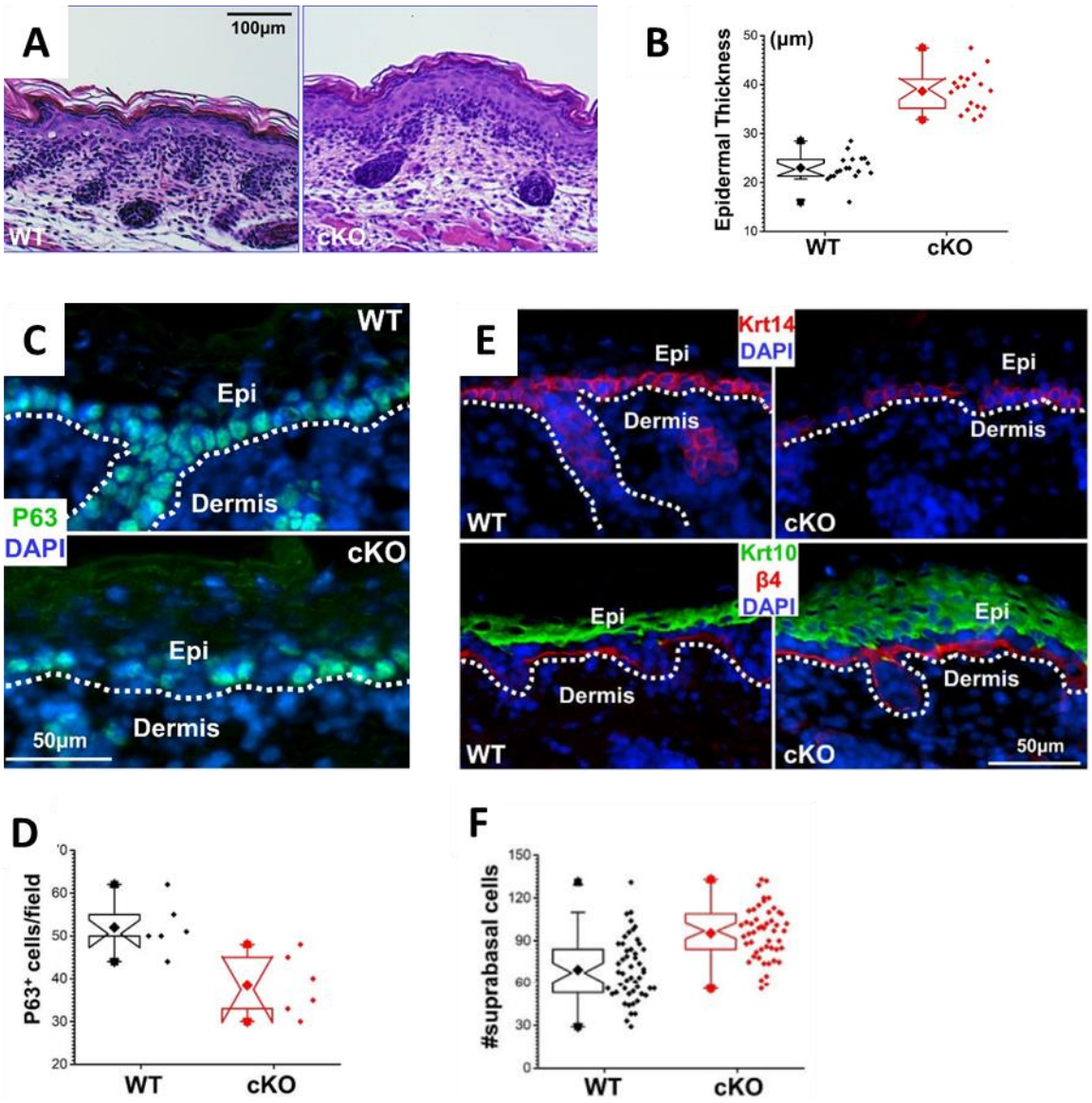

Figure 2.2: ***Mettl14*** **regulates skin homeostasis. A.** HE staining of newborn pup skin sections from WT and *Mettl14* cKO mice. **B.** Quantification of epidermal thickness. **C.** Expression of p63 in skin epidermis was examined by immunofluorescence staining in WT and cKO mice. **D.** Quantification of P63+ cells. **E.** Skin stratification in WT and cKO skin was determined by immunofluorescence staining with different antibodies as indicated. Krt14: Keratin 14; Krt10: Keratin 10; β4: β4-integrin; DAPI for nucleus staining. The dashed line denotes the basement membrane that separates dermis and epidermis (Epi). **F.** Quantification of differentiated suprabasal cells. The box and whisker plots in **B**, **D**, **F** show the mean (solid diamond within the box), 25th percentile (bottom line of the box), median (middle line of the box), 75th percentile (top line of the box), 5th and 95th percentile (whiskers), 1st and 99th percentile (solid triangles) and minimum and maximum measurements (solid squares). n=9 (biological repeats), $P<0.01$ (Student's t-test).

Wounding in skin can mobilize quiescent epidermal progenitor cells for proliferation and migration. To circumvent the issue of perinatal lethality in *Mettl14* cKO animals, we bred the *Metttl14*$^{fl/fl}$ mice with transgenic mice carrying the *K14-Cre-ERT2* allele[116,127]. The resultant inducible cKO animals can grow to adulthood with no apparent changes in skin epidermis or hair coat. However, when challenged by skin injury after administration of tamoxifen, *Mettl14* cKO skin exhibited a significant delay in repairing full-thickness wounds as compared to WT skin (**Figure 2.3 A, B**). Histological analysis revealed that the area of hyperproliferative epithelium that typically proliferates and migrates into the wound site was significantly diminished following injury (**Figure 2.3 C**). Wound-induced hyperproliferation of epidermal cells was also inhibited in cKO skin (**Figure 2.3 D**). Together, these results strongly suggest that m^{6}A modification of RNA mediated by Mettl14 plays a critical role in skin tissue homeostasis and wound repair in vivo.

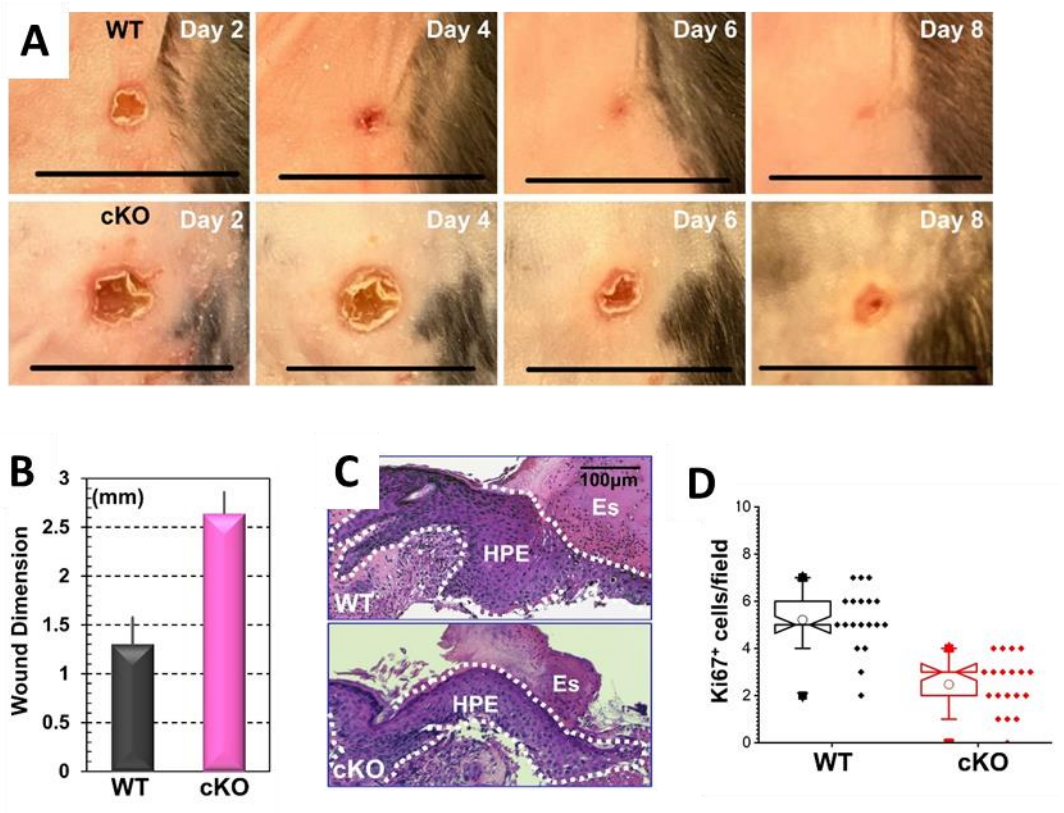

Figure 2.3: **Mettl14 regulates wound healing. A.** Representative images of skin wounds in WT and cKO animals at different time points. Scale bars represent 25mm. **B.** Wound healing as monitored by wound size 8 days post injury. n=3; P<0.01 (Student's t-test). Error bar represents SD (standard deviation). **C.** Histological staining of skin sections at the wound edges. Halves of wound sections are shown. Note significant reduction of HPE (hyperproliferative epidermis) in cKO skin. Es: eschar. Dotted lines denote epidermal boundaries. **D.** Quantification of Ki67-positive cells present in wound HPE, shown in a box and whisker plot. The plot indicates the mean (solid diamond within the box), 25th percentile (bottom line of the box), median (middle line of the box), 75th percentile (top line of the box), 5th and 95th percentile (whiskers), 1st and 99th percentile (solid triangles) and minimum and maximum measurements (solid squares). n=19, P<0.01 (Student's t-test).

Mettl14 **loss impairs epidermal stemness**

Although wound-induced hyperproliferation in adult epidermis is inhibited upon ablation of *Mettl14*, epidermal proliferation, as measured by ki-67 staining, is not significantly affected in the newborn skin of cKO mice (**Figure 2.4 A**). Potential markers for long-term epidermal progenitor cells are not clearly defined in vivo, and different models have been proposed for epidermal tissue maintenance[6,128-137]. However, accumulating evidence reveals the existence of distinct basal cell populations with hierarchical organization and proliferation dynamics in skin epidermis, including slow-cycling progenitor cells and committed progenitor cells with limited proliferative potential[128-133,138]. With classical label-retaining analysis (**Figure 2.4 B**), we found that loss of Mettl14 in skin leads to a dramatic decrease in the number of slow cycling, label retaining cells in the basal layer (**Figure 2.4 C, D**). Upon culture in vitro, primary epidermal keratinocytes will generate three different types of colonies, named holoclones, meroclones, and paraclones, with only holoclones containing undifferentiated epidermal progenitor cells[139-141]. Deletion of *Mettl14* led to a dramatic reduction in the number of holoclones when primary cells were cultured on 3T3 feeder layers (**Figure 2.4 E**). Whereas WT holoclone cells are typically small and tightly packed with undifferentiated morphology, the KO colonies usually have cells that are large and multinucleated with senescent or differentiated morphology (**Figure 2.4 F**). Immunoblots confirmed loss of Mettl14 expression in KO cells. Expression of p63 was also significantly reduced in KO cells (**Figure 2.4 G**). When passaged in vitro, the

KO cells proliferate slower with significantly longer doubling time (**Figure 2.4 H**) and reduced EdU (5-ethynyl-2'-deoxyuridine) incorporation (**Figure 2.4 I**) compared with WT controls. All of this evidence suggests that epidermal stem cells are functionally impaired following *Mettl14* deletion.

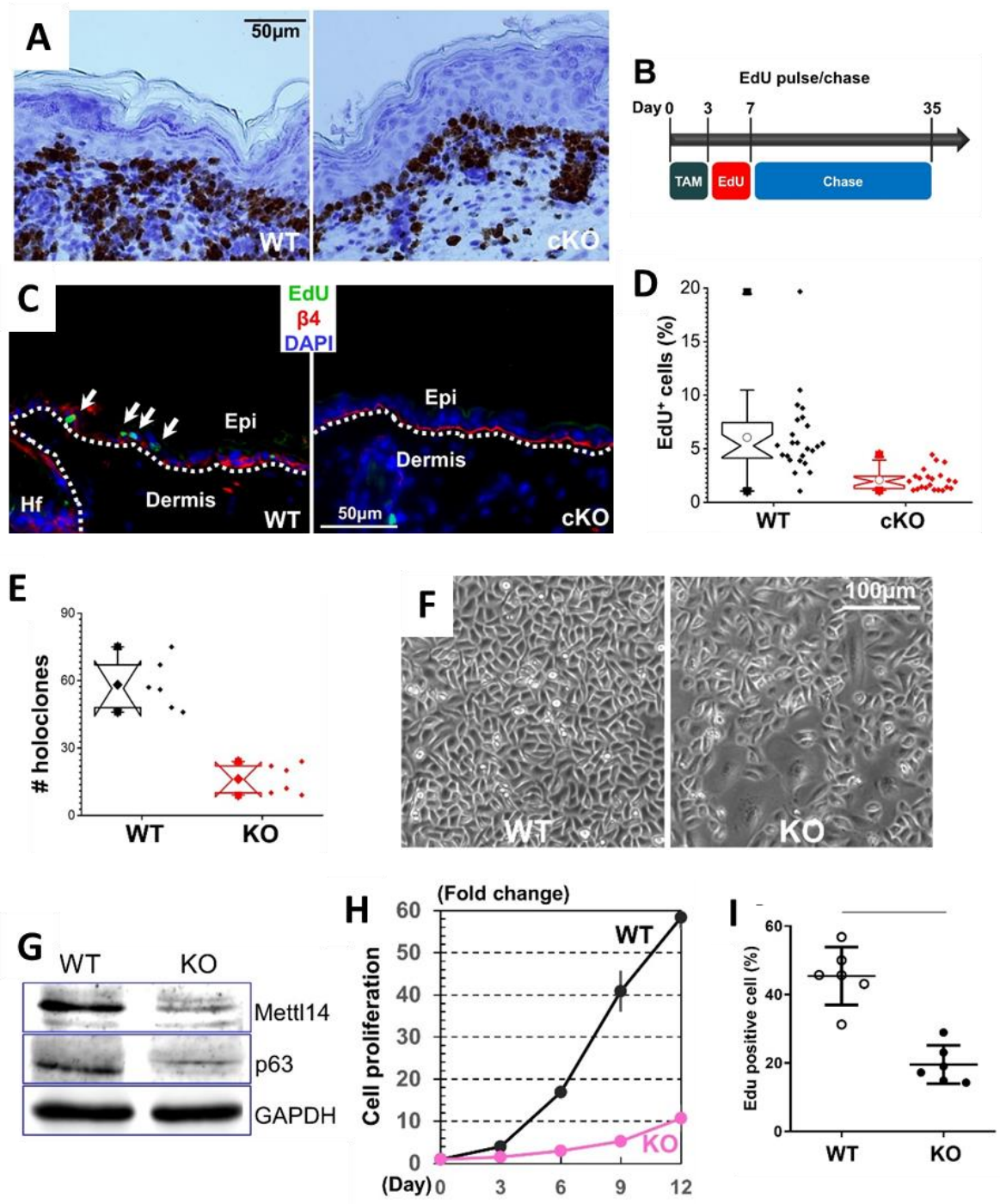

Figure 2.4: **Mettl14 depletion leads to epidermal stem cell loss. Continued on next page.**

Figure [2.4], continued. A. Immunohistochemistry staining shows similar epidermal proliferation in WT and *Mettl14* cKO skin. **B.** Schematic depiction of the design of EdU (5-ethynyl-2'-deoxyuridine) pulse-chase experiments. **C.** EdU staining of WT or *Mettl14* cKO skin after pulse-chase labeling. Skin samples were counterstained with antibody against β4-integrin. Note reduced EdU label-retaining cells in cKO skin epidermis. **D.** Quantification of label-retaining cells in WT or *Mettl14* cKO skin. n=19, P<0.01 (Student's t-test). **E.** Quantification of the number of holoclones derived from WT and *Mettl14* cKO skin. n=24, P<0.01 (Student's t-test). **F.** Morphology of primary keratinocytes isolated from WT or *Mettl14* cKO skin. **G.** Expression of Mettl14 and p63 in WT and KO cells was determined by immunoblots with respective antibodies. Immunoblot for GAPDH was used as loading control. **H.** Proliferation of WT and *Mettl14* null cells in vitro was quantified and shown in a dot plot. n=3, P<0.01 (Student's t-test) for Day 6, 9, and 12, and P<0.05 (Student's t-test) for Day 3. Error bar represents SD. **I.** EdU incorporation assay shows reduced proliferation capability of *Mettl14* null cells in vitro. n=6; P<0.01 (Student's t-test). The box and whisker plots in **D** and **E** show the mean (solid diamond within the box), 25th percentile (bottom line of the box), median (middle line of the box), 75th percentile (top line of the box), 5th and 95th percentile (whiskers), 1st and 99th percentile (solid triangles) and minimum and maximum measurements (solid squares).

To further investigate the change in epidermal stemness, we carried out two additional classical stem cell assays. We first tested the colony forming efficiency (CFE) of the epidermal progenitor cells by culturing the cells at a very low density (100 cell/cm^2) and allowing the colony to form over 7 days. As expected, CFE was markedly decreased upon loss of *Mettl14* (**Figure 2.5 A, B**). More importantly, re-expression of WT *Mettl14* but not the *Mettl14-R298P* mutant that is deficient in methyltransferase activity[142], can restore the CFE in vitro (**Figure 2.5 C**), which suggests that the CFE of epidermal stem cells is dependent on Mettl14 activity. We next carried out a clonal competition and lineage trace analysis[143] using our skin organoid culture and transplantation model[144,145]. As Mettl14-deficient cells failed to sustain long-term

culture in vitro, we isolated primary epidermal keratinocytes from the inducible *Mettl14* KO strain. Before treatment with tamoxifen, the inducible KO cells and their WT counterparts grew at a similar rate. To monitor their epidermal regeneration capacity and trace their fate upon engraftment, we transduced the WT and inducible KO cells with lentivirus encoding either H2B-RFP or H2B-GFP. Fluorescently labeled cells were mixed at a 1:1 ratio to generate skin organoids. Interestingly, whereas clone size measurement with fluorescent microscopy revealed no significant changes between WT and inducible KO cells before tamoxifen treatment, induction of Cre recombination with tamoxifen led to continual loss of *Mettl14* KO cells in the skin, which became barely detectible 14 days after tamoxifen treatment (**Figure 2.5 D, E**). These results indicate that Mettl14 is essential for maintaining epidermal stemness.

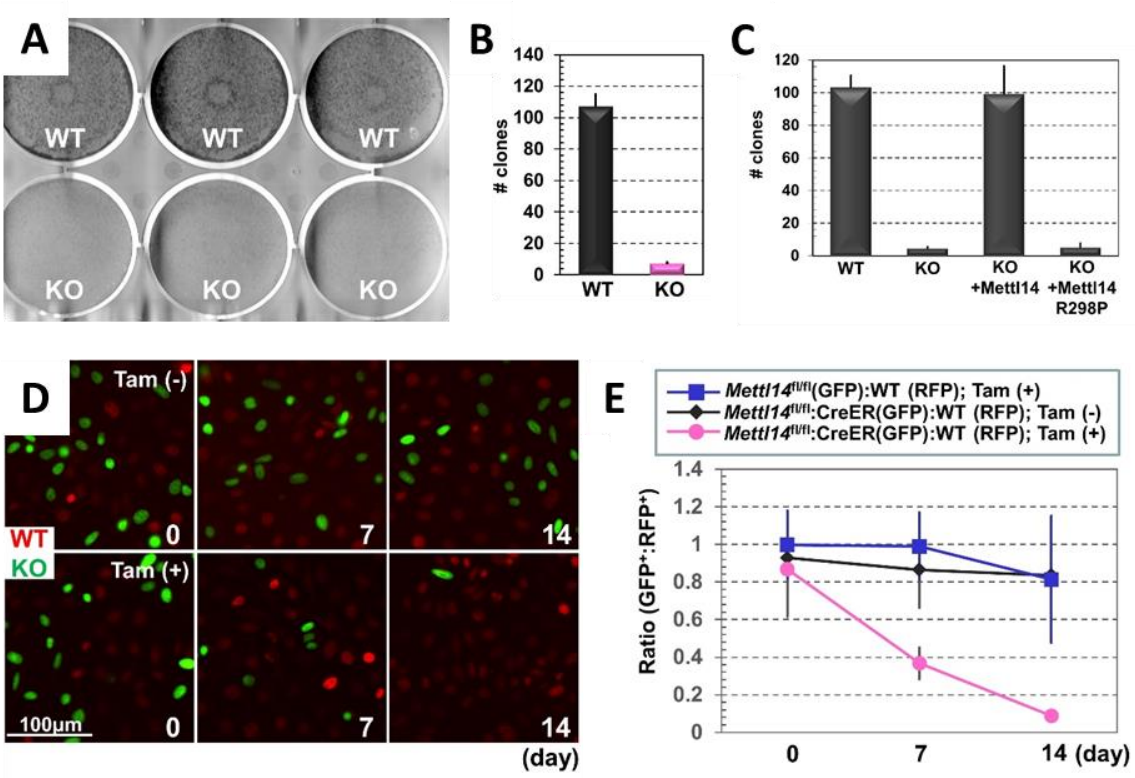

Figure 2.5: Mettl14 is required for maintaining epidermal stemness. Continued on next page.

Figure [2.5], continued. A. CFE (colony formation efficiency) of WT and *Mettl14* null cells was determined in vitro. **B.** Colonies from each well are quantified and shown in a bar graph. n=19, P<0.01 (Student's t-test). Error bar represents SD. **C.** CFE (colony formation efficiency) of WT, *Mettl14* KO, and *Mettl14* KO cells with re-expression of *Mettl14* or *Mettl14-R298P* mutant was determined in vitro. Error bar represents SD. **D.** Fluorescence microscopy demonstrates different survival capability of WT and inducible *Mettl14* KO cells with or without Tamoxifen (TAM) treatment. **E.** Ratio of WT and inducible *Mettl14* KO cells in the co-culture model was quantified and shown in dot plots for KO cells with TAM treatment compared with WT cells or KO cells without TAM stimulation at both Day 7 and 14. Error bar represents SD. n=8, P<0.01 (Student's t-test).

RNA N^6-methyladenosine sequencing and Gene Ontology analysis

To uncover how changes in the RNA methylomes regulate epidermal stem cell self-renewal and differentiation, we performed m^6A sequencing (m^6A-seq) and RNA sequencing (RNA-seq) of polyadenylated RNAs isolated from undifferentiated epidermal progenitor cells and from epidermal progenitor cells with induced differentiation via calcium shift[146]. Our profiling identified 7,379 and 6,945 RNA species with m^6A modifications in progenitor cells and differentiated cells, respectively. Among them, 260 RNAs have markedly reduced m6A modification upon differentiation (fold change > 2), whereas 1,474 RNAs have elevated levels of m^6A modification. GO (Gene Ontology) term enrichment analysis of RNAs with altered m^6A modification revealed a variety of enriched clusters following keratinocyte differentiation (**Figure 2.6 A, B**), including annotations pertaining to RNA processing and binding.

Long non-coding RNAs (lncRNAs) have emerged as an important class of regulators involved in many processes, including skin development and homeostasis[26,28]. Our analysis

revealed substantially altered m^6A modifications of different lncRNAs during skin differentiation, including Gas5 (growth arrest-specific 5), Neat1 (nuclear enriched abundant transcript 1), Malat1 (metastasis-associated lung adenocarcinoma transcript 1), Snhg18 (small nucleolar RNA host gene 18) and Pvt1 (Plasmacytoma variant translocation 1) (**Figure 2.6 C**). Our analyses point towards an intriguing possibility that m^6A modification on lncRNA may act as an important regulator of epidermal stemness.

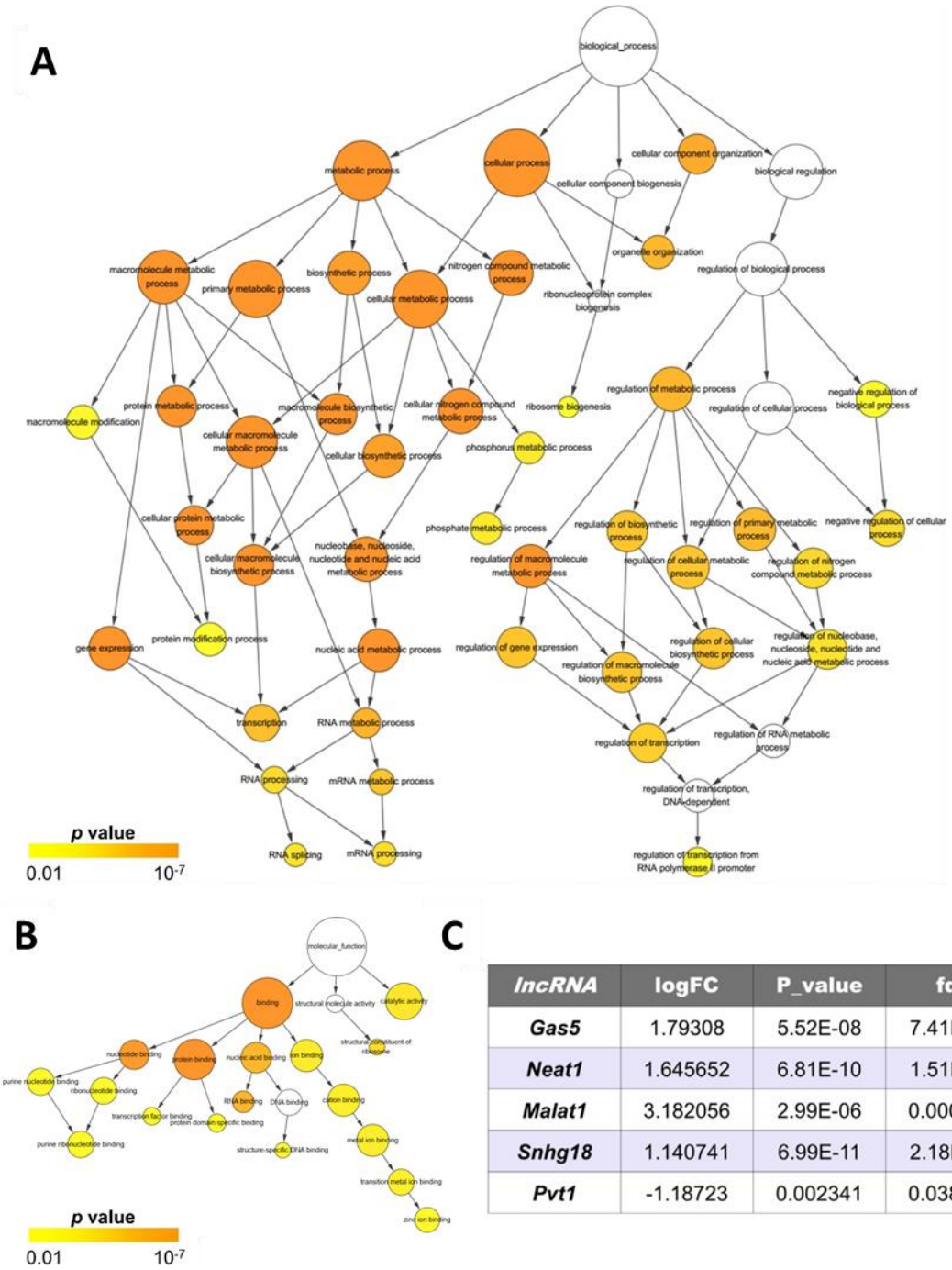

lncRNA	logFC	P_value	fdr
Gas5	1.79308	5.52E-08	7.41E-06
Neat1	1.645652	6.81E-10	1.51E-07
Malat1	3.182056	2.99E-06	0.000215
Snhg18	1.140741	6.99E-11	2.18E-08
Pvt1	-1.18723	0.002341	0.038082

Figure 2.6: Mapped enrichment results from RNA methylome profiling. A. Transcripts with at least a two-fold decrease in m^6A level in differentiated versus undifferentiated cells were analyzed and visualized for overrepresented GO Biological Process terms using Cytoscape with Bingo plugin. Nodes represent gene sets with shared enrichment annotation. Diameter of nodes correspond to the number of genes associated with enrichment term. The color of the node represents the corrected p value. White nodes are not over-represented, whereas colored nodes are over-represented. **B.** Analysis for overrepresented GO Molecular Function terms using the same method as in **A**. **C.** Profiling of RNA methylome by m^6A-seq shows significant changes in lncRNA modifications upon epidermal differentiation in vitro.

DISCUSSION

Defects in skin epidermal differentiation or wound repair can result in dire consequences for our survival because the skin provides an essential barrier protecting us against many different types of environmental damage[2,141]. Tissue homeostasis and regeneration of our skin are driven by the epidermal basal progenitor cells and are controlled by the critical balance between cell proliferation, cell differentiation, and cell death. Stemness and differentiation of epidermal progenitor cells are controlled by a complex and choreographed signaling network; however, the complexity of the multilevel regulation of these processes remains ill defined.

RNA m^{6}A modification has been uncovered as one of the most important mechanisms of regulating RNA post-transcriptionally. The m^{6}A proteins, including writers, erasers, and readers, are highly conserved across a wide range of species, both in prokaryotes and eukaryotes[147]. The m^{6}A machinery is especially important for embryonic stem cell development, as it provides a means for rapid turn-over of transcriptome and facilitates change in cell fate[84]. Conversely, dysregulated m^{6}A pathway has been implicated in a wide range of cancers, including acute myeloid leukemia[101] and glioblastoma[104].

We probed the role of m^{6}A modification in epidermal development by conditionally ablating *Mettl14*, one of the main m^{6}A writer proteins, in epidermal cells. We found that loss of m^{6}A modification led to significant disruption of epidermal development, including loss of the basal stem cell population, and abnormal proliferation of differentiated cells at the

suprabasal layer. Importantly, *Mettl14* knockout also led to significant defects in skin wound healing, indicating an inability of epidermal stem cells to proliferate and mobilize under tissue stress.

Mettl14 cKO mice also showed defects in hair follicle formation shortly after birth. In the skin sections from newborn cKO pups, the hair follicles are deformed and are fewer in number. During embryogenesis, hair follicle development initiates with the "first dermal signal", which induces the placode to form in the epidermis at E14.5[148]. The placode then continues to expand downward and differentiate to form the hair shaft. The epidermis thus contributes to hair follicle development in two important ways. First, the dermal-epidermal cross talk between E14.5-E15.5 is essential for the placode to develop into germ and peg. Second, the epidermal stem cells need to migrate downwards and differentiate into the hair follicle epithelium at E18.5[149]. It is thus likely that RNA m^6A modification may play a role during one or both of these processes. Future studies will be needed to determine the precise role of RNA m^6A modification in hair development.

We also observed that a significant number of *Mettl14* cKO pups die prematurely, usually around day 3-5 after birth. Abnormal skin development can impair the barrier function of the skin, leading to increased susceptibility to environmental hazards or excessive water loss through the skin[150]. We examined the barrier function of the pups using a toluidine blue penetration test[151], but found no evidence of impaired skin permeability in the cKO pups. In

our *Mettl14* cKO mice, expression of *Cre* recombinase is driven by the *K14* promoter, which is expressed in the epidermis during development. However, *K14* is also expressed in esophageal epithelium during development, and malformation of the esophagus can also lead to malnutrition and premature death. We microscopically examined sections taken from the esophagus of newborn *Mettl14* cKO pups, but also did not find any abnormality. The precise reason for early mortality in our *Mettl14* cKO remains to be identified. Our preliminary investigation is also insufficient to completely rule out defects in barrier function or esophageal malformation as a cause. More sensitive studies may be needed, such as transepithelial water loss (TEWL) measurement or ultrastructure microscopy.

On the cellular level, the EdU incorporation assay revealed that the *Mett14* cKO mice are almost devoid of the slow-cycling quiescent stem cell population in the basal epidermis. The *Mettl14* cKO epidermal progenitor cells also grew at a significantly slower rate in vitro, and failed to from colonies when plated at low density. Finally, the *Mettl14* cKO epidermal progenitor cells were also out-competed when co-cultured with WT cells. These well-established stem cell assays all point to the same conclusion: that Mettl14 is critical in maintaining epidermal stemness.

The molecular and cellular functions of RNA m^6A modification have mostly been explored in the context of embryonic stem cells and cancer cells. However, several studies also highlight the importance of this regulatory mechanism in development and adult tissue

homeostasis. Interestingly, studies on RNA m^{6}A modification in neuronal development reveal findings strikingly similar to ours. Specifically, mice with conditional knockout of *Mettl14* in neuronal stem cells show a significant decrease in neuronal stem cell proliferation, as well as premature differentiation[88]. In addition, the differentiated neuronal cells still retain normal identity. In our model, although there is a significant reduction in the number of epidermal stem cells in the basal layer accompanied by an increased number of differentiated cells in the suprabasal layer, the differentiated cells can still migrate upward and constitute the spinous layer, granular layer, and corneal layer without apparent disorder or functional impairment. This suggests that like neuronal stem cells, the main role of RNA m^{6}A modification is regulating stem cell self-renewal as opposed to directing differentiation. However, the mechanisms by which m^{6}A modification regulates stem cell self-renewal in neuronal stem cells and epidermal stem cells are different. In the neuron, m^{6}A modification regulates histone modification by destabilizing transcripts of histone modifiers, such as CBP and p300[88]. In contrast, our m6A-seq data did not reveal prominent changes in histone modification transcripts between undifferentiated and differentiated epidermal progenitor cells. Instead, our Gene Ontology analysis suggests that m^{6}A regulation may affect epidermal stemness through lncRNAs.

Protein coding regions comprise only 1-2% of our genome, and a major component of the noncoding genome are lncRNAs. Compared with mRNAs, lncRNAs usually have a relatively

low expression level but strong tissue-specific patterns. Although nearly 28,000 lncRNAs have been cataloged in the human genome, most lncRNAs have not been functionally characterized. To date, only a few lncRNAs have been identified as playing an important role in epidermal stemness and homeostasis with cultured human primary keratinocytes or human skin tissue samples as model systems, including DANCR (differentiation antagonizing non-protein-coding RNA)[27], TINCR (terminal differentiation-induced noncoding RNA)[28], PRANCR (progenitor renewal associated noncoding RNA)[32], SMRT-2 (SCC mis-regulated transcripts-2)[29], and uc.291 (UC-containing lncRNA)[152]. Consistent with previous reports[27], our RNA-seq revealed a significant decrease in ANCR transcript level upon calcium-induced differentiation of mouse epidermal progenitor cells. However, contradictory to the role of TINCR in promoting epidermal differentiation[28], transcripts of *Gm20219*, the mouse homolog of *TINCR*, is significantly reduced in differentiated mouse keratinocytes. It is noteworthy that lncRNAs are less sequence-conserved compared with protein-coding RNAs, and many functional lncRNAs are human- or primate-specific. It is likely that Gm20219 and TINCR may function in a different manner in mouse and human epidermal cells. Neither ANCR nor TINCR shows significant changes in m^6A modifications upon epidermal differentiation, suggesting their functions are regulated by different mechanisms in skin epithelial cells.

Data analysis from our m^6A-seq data revealed five lncRNAs with significant changes in m^6A modification level upon epidermal differentiation, including Gas5, Neat1, Malat1, Snhg18,

and Pvt1. Curiously, none of the five lncRNAs have been studied in epidermal cells, but have all been implicated to play a role in cancer. Three of the lncRNAs, Gas5, Malat1, and Pvt1, have been reported to be regulated through m^6A modification in cancer cells. RNA m^6A modification on Gas5 facilitates its degradation through the m^6A reader YTHDF3. In contrast, Malat1-m^6A is recognized by another reader, YTHDC1, to regulate nuclear speckle formation. From our sequencing analysis, *Gas5* transcript level did not change with its methylation status. We also did not find significant changes in nuclear speckle formation from microscopy and ultra-microscopy observation in epidermal cells before and after differentiation. This suggests that Gas5 and Malat1 methylation may not play an important role in epidermal regulation, though it is still possible they may act through a different mechanism than cancer cells. Pvt1 is another interesting candidate, because Pvt1 has been shown to interact with and stabilize MYC in cancer cells, and it acts as an oncogene in this manner. In osteosarcoma cells, Pvt1 has been found to be demethylated by ALKBH5 to decrease YTHDF2-mediated degradation, suggesting that Pvt1 is also regulated by m^6A modification[153]. Since MYC is not only over-expressed in a wide range of cancers, but is also one of the master regulators of epidermal homeostasis, the potential interaction between Pvt1 and MYC in epidermal stem cells is of particular interest for further investigation.

CHAPTER III

RNA N6-METHYLADENOSINE MODIFICATION ENHANCES PVT1-MYC INTERACTION AND INCREASES MYC STABILITY

INTRODUCTION

Epidermal homeostasis is maintained by epidermal stem cells located in the basal layer. The epidermal stem cells are constantly challenged to make a decision: to remain dormant; to proliferate, which will replenish the stem cell population; or to differentiate, which can replenish the functional cells in the upper layers. This decision is orchestrated by a host of control mechanisms and is achieved through genetic as well as epigenetic means. In the previous chapter, we demonstrated that an additional layer of epidermal stem cell control is governed at the transcriptomic level, specifically, via RNA m^6A modification. Through an m^6A-sequencing approach, we identified several potential long non-coding RNAs (lncRNAs) that are modified by m^6A during skin differentiation.

We decided to focus on Pvt1, one of the lncRNAs identified in our sequencing results. The main rationale is that Pvt1 is the only lncRNA that shows a decreased methylation level after induced epidermal differentiation, which is consistent with the decreased expression of Mettl14 and global reduction in RNA methylation observed in differentiated cells. Additionally, Pvt1 is a very attractive target because it has been found to be up-regulated in many cancers and has been proposed to possess oncogenic properties via binding and stabilizing the

oncoprotein MYC[154]. Because MYC is also one of the master regulators of epidermal stemness, we hypothesized that m^{6}A modification is required for Pvt1-MYC interaction and that loss of m^{6}A leads to decreased MYC level and epidermal differentiation.

Using CRISPR-Cas9 (Clustered Regularly Interspaced Short Palindromic Repeats-CRISPR-associated protein 9) mediated *Pvt1* knockout, we were able to demonstrate that Pvt1 is indeed required for epidermal stemness and that its function is dependent on m^{6}A modification on Pvt1. We were able to further show that loss of Pvt1 m^{6}A modification leads to decreased MYC interaction as well as rapid MYC degradation in vitro. In addition, the loss of epidermal stemness observed in the *Mettl14* knockout cells can be rescued by expressing MYC externally, both in cell culture and in skin organoids. These results strongly support our hypothesis that m^{6}A modification of Pvt1 enhances its interaction with MYC, which stabilizes MYC and maintains epidermal stemness.

MATERIALS AND METHODS

Antibodies and chemical reagents

P63 antibody was obtained from Genetex (Irvine, CA). Mettl14 antibody was obtained from Sigma (St Louis, MO). MYC, GAPDH, and α-tubulin antibodies were obtained from ProteinTech (Rosemont, IL). HA-conjugated beads and HA antibodies were obtained from Sigma (St. Louis, MO). Rabbit polyclonal antibodies against Ki67 were obtained from Santa

Cruz Biotechnology, Inc. (Santa Cruz, CA). Other chemicals or reagents were obtained from Sigma, unless otherwise indicated.

Cell culture

Primary mouse keratinocytes were isolated from the epidermis of newborn mice using trypsin after prior separation of the epidermis from the dermis by an overnight dispase treatment. Keratinocytes were plated on mitomycin C–treated 3T3 fibroblast feeder cells until passage three. Cells were cultured in E-media supplemented with 15% serum with a final concentration of 0.05 mM Ca^{2+}.

Protein biochemical analysis

Western blot was performed as described previously[117]. Cell lysates were prepared with RIPA (radioimmunoprecipitation assay) buffer (50 mM HEPES, pH 7.4, 150 mM NaCl, 10% Glycerol, 1.5 mM MgCl2, 1 mM EGTA, 1% Triton X-100, 1% Sodium Deoxycholate, 0.1% SDS) containing protease inhibitors and phosphatase inhibitors. Equal amounts of the cell lysates were separated using SDS-polyacrylamide gel electrophoresis (PAGE) and electroblotted onto a nitrocellulose (NC) membrane. The immunoblot was incubated with Odyssey blocking buffer (Li-Cor) at room temperature for 1 hour, followed by an overnight incubation with the primary antibody. Blots were washed three times with Tween 20/Tris-buffered saline (TBST) and incubated with a 1:10,000 dilution of secondary antibody for 1 hour at room temperature. Blots were washed three times with TBST. Visualization and

quantification were carried out with the LI-COR Odyssey scanner and software (LI-COR Biosciences, Nebraska, USA).

RNA extraction and quantitative RT–PCR

Total RNA was isolated with TRIzol reagent (Invitrogen) using Direct-zol kit (Zymo Research). mRNA was extracted from the total RNA using a Dynabeads mRNA purification kit (Invitrogen). mRNA concentration was measured by ultraviolet absorbance at 260 nm. For analysis of mRNA expression, 200–500 ng of RNA was reverse-transcribed into cDNA using the High-Capacity cDNA Reverse Transcription kit (Applied Biosystems). Quantitative realtime PCR analysis was then performed using PerfeCTa SYBER green Supermix (Quantabio) on the StepOnePlus RT–PCR system (Thermo Fisher Scientific). GAPDH or ACTB was used as endogenous control. Each sample was run in triplicate.

Quantification of RNA m6A methylation via m^6A-immunoprecipitation

Protein G Dynabeads (Thermo Scientific) were washed and resuspended in immunoprecipitation (IP) buffer containing 20 mM Tris (pH 7.4), 750 mM NaCl, and 0.5% NP40. Next, m^6A antibody (New England Biolabs) was added to the beads and incubated for 30 min at 4°C. After incubation, the supernatant was removed and washed with IP buffer, then purified RNA was added and incubated for 1 hour at 4°C. The beads were then washed with

low salt buffer containing 10 mM Tris (pH 7.4), 10 mM NaCl, 0.1% NP40, followed by a second wash with high salt buffer containing 10 mM Tris (pH 7.4), 500 mM NaCl, 0.1% NP40. Finally, the RNA was eluted with RLT buffer (Qiagen) and further purified using the RNA Clean and Concentrator-5 kit (Zymo Research). The relative level of m6A-modified RNA was quantified via RT–PCR as described in the previous section.

Quantification of Pvt1-MYC interaction via MYC-immunoprecipitation

Cell lysate was collected from transfected 293 cells expressing MYC with HA tag. 50 µl anti-HA agarose beads (Peirce) were added to the lysate and incubated at 4°C for 1 hour. After incubation, the beads were washed with RNA–protein binding buffer containing 25 mM Tris (pH 7.4), 150 mM KCl, 5 mM EDTA, 0.5 mM DTT, 0.5% NP40, and SUPERNase (Invitrogen) 0.1 U/µl. Next, purified RNA was added to the MYC-HA beads and incubated for 2 hours at 4°C. Finally, the beads were washed with RNA–protein binding buffer and the RNA was purified using the RNA Clean and Concentrator-5 kit (Zymo Research). The relative level of MYC-bound Pvt1 was determined by RT–PCR as described in the previous section.

FTO demethylation of RNA

Removal of m^6A methylation of mRNA and lncRNA was performed as previously described[64]. In brief, 200 ng of polyadenylated RNA purified from cultured cells was incubated

with 2 μM purified FTO in a 20 μl reaction system. The reaction buffer was composed of 50 mM HEPES buffer (pH6.5), 100 mM KCl, 2 mM $MgCl_2$, 2 mM L-ascorbic acid, 300 μM α-ketoglutarate, 150 μM $(NH4)_2Fe(SO4)_2$•6H2O, and SUPERNase (Invitrogen) 0.2 U/μl. After 1 hour of incubation, the reaction was quenched by adding 5 mM EDTA. For the control group, EDTA was added prior to incubation. The demethylated RNA was purified using the RNA Clean and Concentrator-5 kit (Zymo Research).

Skin organoid culture and grafting

Skin organoid culture and grafting has previously been performed in our lab and described[144,145]. In brief, decellularized dermis (1 cm × 1 cm) was prepared from newborn CD1 mice. 1.5×10^6 cultured keratinocytes were seeded onto the dermis in a cell culture insert. After overnight attachment, the skin culture was exposed to air/liquid interphase. To transplant the graft to 8-12 week old nude mice (Jackson lab, *Nu/J* strain), two 1 cm × 1 cm wounds were introduced on the back skin. After transplantation, the wound edge was sealed with surgical glue. The grafted animals were housed separately, and the wound bandages were usually removed 1 week post-surgery. All the experiments included more than three biological replicates (independent skin grafts). For phenotypic analysis, at least three sections were taken from each graft for analysis and quantification by staining.

Histology and immunostaining

For FFPE (formalin-fixed paraffin-embedded) tissue, skin samples were fixed in 10% formalin for 24 hours, then dehydrated via xylene exchange overnight and embedded in paraffin. 0.5 μm sections were made and stained with HE (hematoxylin and eosin). For immunohistochemistry staining (IHC), sections were stained on a Leica Bond RX automatic stainer. Epitope retrieval solution II (Leica Biosystems, AR9640) was used for 20 minute heat-induced antigen retrieval (HIAR). Antibodies were applied on tissue sections for 60 minutes of incubation and the antigen-antibody binding was detected using Bond polymer refine detection (polymer HRP, Leica Biosystems, DS9800). For quantification, slides were inspected under the microscope at high power (400x magnification) and epidermal cells were counted manually by a trained pathologist.

For frozen sections, skin samples were embedded in Tissue-Tek OCT compound (Sakura) and 0.7 μm sections made on a cryostat. The sections were fixed in 10% formalin and stained with HE. For immunofluorescence staining (IF), sections were fixed in 4% paraformaldehyde, permeabilized in 0.1% Triton X100 and blocked in blocking solution (2.5% normal goat serum, 2.5% normal donkey serum, 2% gelatin, 0.1% Triton X100 and 1% bovine serum albumin in PBS).

MYC protein stability assay

Primary keratinocytes were treated with 20 nM cycloheximide (CHX). Whole cell lysates were collected at 0, 30, 60, 90, 120, 180, and 300 min post-CHX treatment and subjected to immunoblotting with MYC antibody, as described in the previous section. Band intensity was determined by densitometry.

Statistical analysis

Statistical analysis was performed using Excel, OriginPro, GraphpadPrism or SciDAVis software. Box plots were used to describe the entire population without assumptions about the statistical distribution. A Student's t-test was used to assess the statistical significance (P value) of the difference for the experiments.

RESULTS

***Pvt1* loss leads to epidermal stemness defect**

Our m^6A sequencing analysis revealed the possibility that m^6A methylation of lncRNAs may drive epidermal stemness. Of the five lncRNAs we identified that showed significant change in m^6A level after induced epidermal differentiation, Pvt1 was the only one with reduced methylation after differentiation, which is consistent with the global RNA methylation pattern in differentiated epidermal cells. We thus hypothesized that Pvt1 m^6A modification is required for epidermal stemness.

While Pvt1 has been previously reported to be m^6A modified, the modification site has not been determined[153]. We first sought to determine the methylation sites on Pvt1. From the m^6A-sequencing data, we were able to identify two m^6A clusters on Pvt1 transcript in exon 2. Next, we matched the consensus m^6A sequence Pu[G>A]m6AC[A/C/U] with the sequence of the two clusters, which revealed five potential m^6A modification sites on Pvt1: A282, A294 and A303 in the first cluster and A446 and A452 in the second. To further evaluate the m^6A modification status of these two clusters, we created mutations at the five putative sites, replacing A (adenosine) with G (guanosine), and measuring the m^6A modification level via m^6A-immunprecipitation followed by RT-PCR on Pvt1. Interestingly, when either one of the clusters was mutated, the Pvt1 m^6A modification level was reduced by approximately 50%, and when both clusters were mutated, Pvt1 methylation was nearly depleted (**Figure 3.1 A**). Thus we confirmed that both of these clusters constitute the dominant m^6A-modifiction site on the Pvt1 transcript.

While several lncRNAs have been implicated in epidermal cell regulation, the role of Pvt1 in skin development has not yet been explored. To this end, we first developed a CRISPR-Cas9 mediated knockout line by targeting two guided RNAs against the complementary sequences at both ends of the lncRNA gene (**Figure 3.1 B**). Interestingly, the *Pvt1* KO cells failed to propagate after selection, suggesting that it is an essential gene for maintaining stemness of epidermal progenitor cells in vitro. To overcome this, we used a doxycycline-inducible

platform to deliver the Cas9 (CRISPR-associated protein 9) protein (iCas9)[155], together with a PiggyBac transposon vector encoding the two gRNAs required for *Pvt1* deletion[156]. In stably transduced cells, induction with doxycycline led to a significant reduction in *Pvt1* expression (**Figure 3.1 C**).

We next evaluated the impact of epidermal stemness on the *Pvt1* knockout cells using colony formation assays. As expected, upon doxycycline-induced knockout of *Pvt1*, the number of colonies dropped significantly compared to WT cells or non-induced cells (**Figure 3.1 D**). As our CRISPR-mediated knockout approach may also result in the potential removal of genetic regulatory elements on *MYC*[157], we tested the change in epidermal stemness using siRNA against Pvt1 transcripts and observed a similar effect (**Figure 3.1 E, F**). This suggests that the stemness defect caused by Pvt1 depletion does not occur at the genomic level, but instead at the transcriptomic level. Importantly, we were able to rescue the colony forming defect by re-introducing WT *Pvt1*, but not the mutant *Pvt1* with all five m^6A-sites mutated (*PVT1-A5G*) (**Figure 3.1 D**). This indicates that not only is Pvt1 essential for epidermal stemness, but its regulatory action is also dependent on m^6A modification.

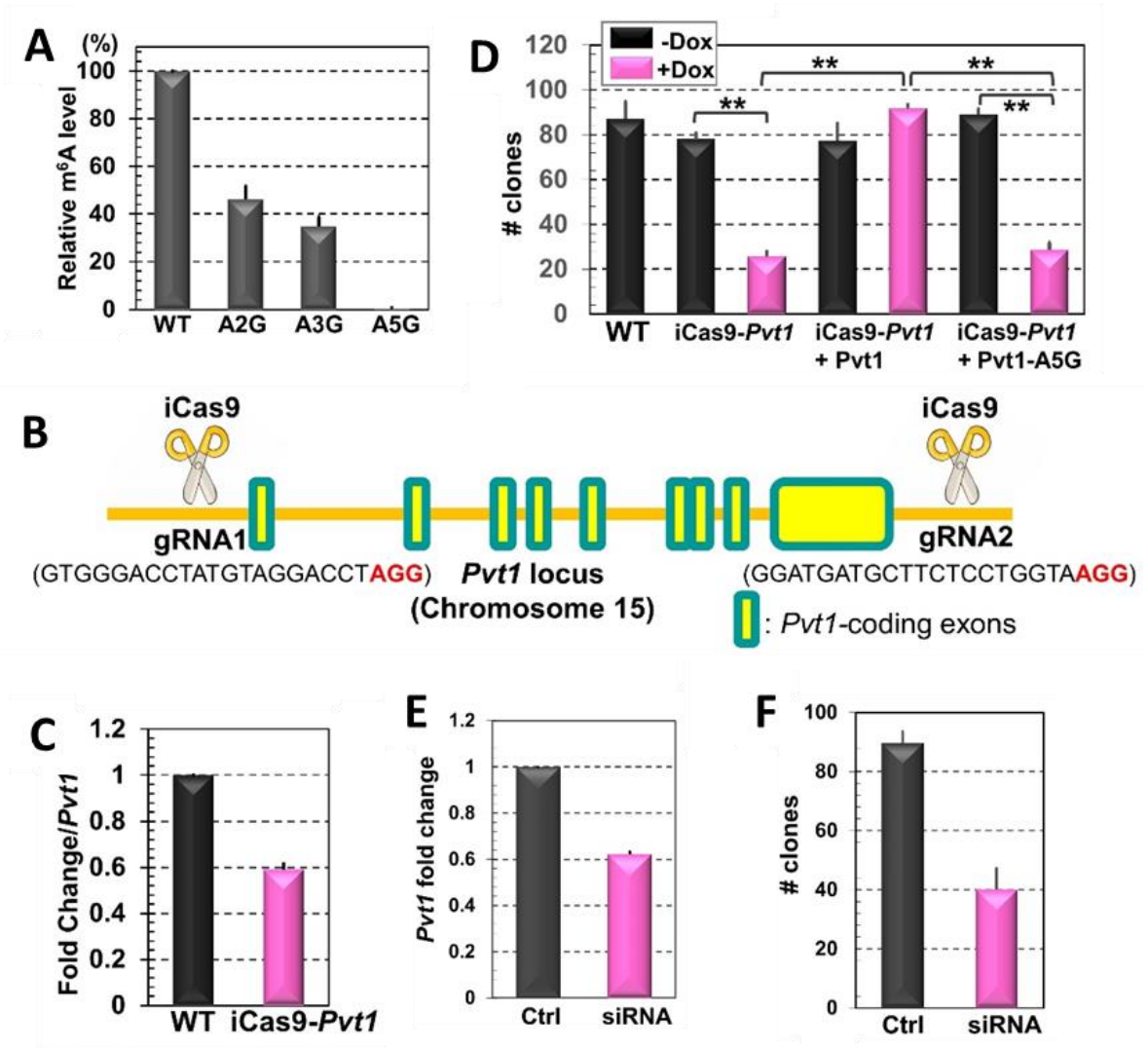

Figure 3.1: Pvt1 m^{6}A modification is required for epidermal stemness. A. Mutations in the predicted m^{6}A modification sites can significantly reduce Pvt1 methylation. **B.** Targeting strategy for deletion of Pvt1 in cultured mouse epidermal progenitor cells. iCas9: inducible Cas9. gRNA: guide RNA. **C.** Deletion of endogenous Pvt1 by an inducible Cas9 (iCas9) system can significantly reduce Pvt1 RNA level. n=3, P<0.01 (Student's t-test). Error bar represents SD. **D.** CFE of WT, Pvt1 inducible KO, and Pvt1 inducible KO cells rescued with WT or mutant *Pvt1* was quantified and presented in a bar graph. n=3, **: P<0.01 (Student's t-test). **E.** Decrease of Pvt1 level upon transfection of siRNA, as determined by RT-PCR. **F.** CFE of WT control cells and cells with *Pvt1* knockdown (siRNA).

Mutation of the m^{6}A-sites on Pvt1 can potentially lead to alterations in the secondary structure of the transcript due to change in base-pairing stability, which may in turn cause changes in Pvt1 function or stability and confound our analysis. To account for this, we performed an in silico analysis to determine the secondary structure of Pvt1 using the RNAfold software[158], and found that three of the five adenosines on the m^{6}A modification sites may potentially be involved in base-pairing (**Figure 3.2 A-C**). To this end, we prepared a Pvt1 mutant with the three corresponding T residuals mutated to C (PVT1-A5GT3C) to preserve base-pairing stability and minimize the potential impact on secondary structure. When the PVT1-A5GT3C mutant was expressed in *Pvt1* knockout cells, it also failed to restore the number of colonies (**Figure 3.2 D**), suggesting that failure of the PVT1-A5G mutant to restore epidermal stemness is due to the mutant's inability to become methylated and not due to to secondary structure changes from the mutation.

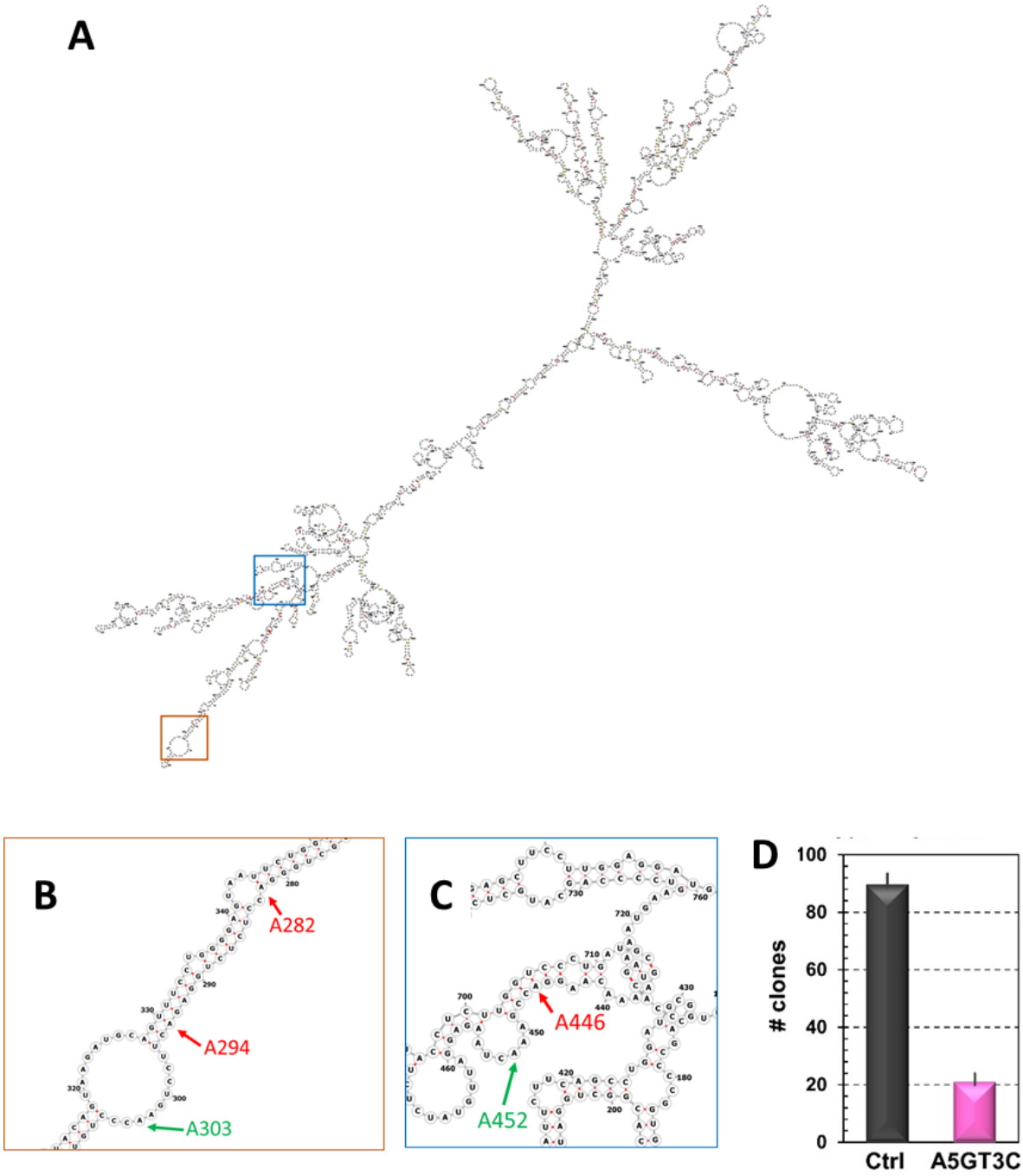

Figure 3.2: Stemness defect in Pvt1-A5G is not due to disruption of secondary structure base-pairing. A. Predicted Pvt1 secondary structure using RNAfold software. Figure was generated using the draw tool RNAstucture (http://rna.urmc.rochester.edu/RNAstructureWeb/). The two clusters with m^{6}A modification are indicated by the brown and blue squares. **B.** First m^{6}A cluster on Pvt1. A282 and A294 are predicted to pair with U345 and U330. **C.** Second m^{6}A cluster on Pvt1. A446 is predicted to pair with U705. **D.** Expression of the Pvt1-A5GT3C mutant, which has the 3 pairing uracils mutated to cytosine, cannot restore CFE in vitro, resembling the effect of the Pvt1-A5G mutant.

Finally, to further confirm that Pvt1 regulates epidermal stemness in vivo, we took advantage of the mouse skin organoid and transplantation model that was recently established by our group[144,145]. Skin organoids derived from WT and inducible *Pvt1* KO cells can both be efficiently grafted to host mice and regenerate skin. However, upon doxycycline administration, the KO skin grafts grew notably thicker with expansion of spinous cells and a decrease in p63-positive basal cells, resembling the phenotypes of *Mettl14* cKO skin. (**Figure 3.3 A-F**).

We further assessed the changes in epidermal stemness using a clonal competition assay. We transduced the WT and inducible *Pvt1* KO cells with lentivirus encoding either H2B-RFP or H2B-GFP and mixed the cells at a 1:1 ratio to generate the skin organoids. Interestingly, induction of Cas9 with doxycycline for *Pvt1* deletion led to continual loss of KO cells in the skin (**Figure 3.3 G, H**). Taken together, our results provide compelling evidence that lncRNA Pvt1 plays an important role in sustaining epidermal stemness, which requires m^6A modification of Pvt1.

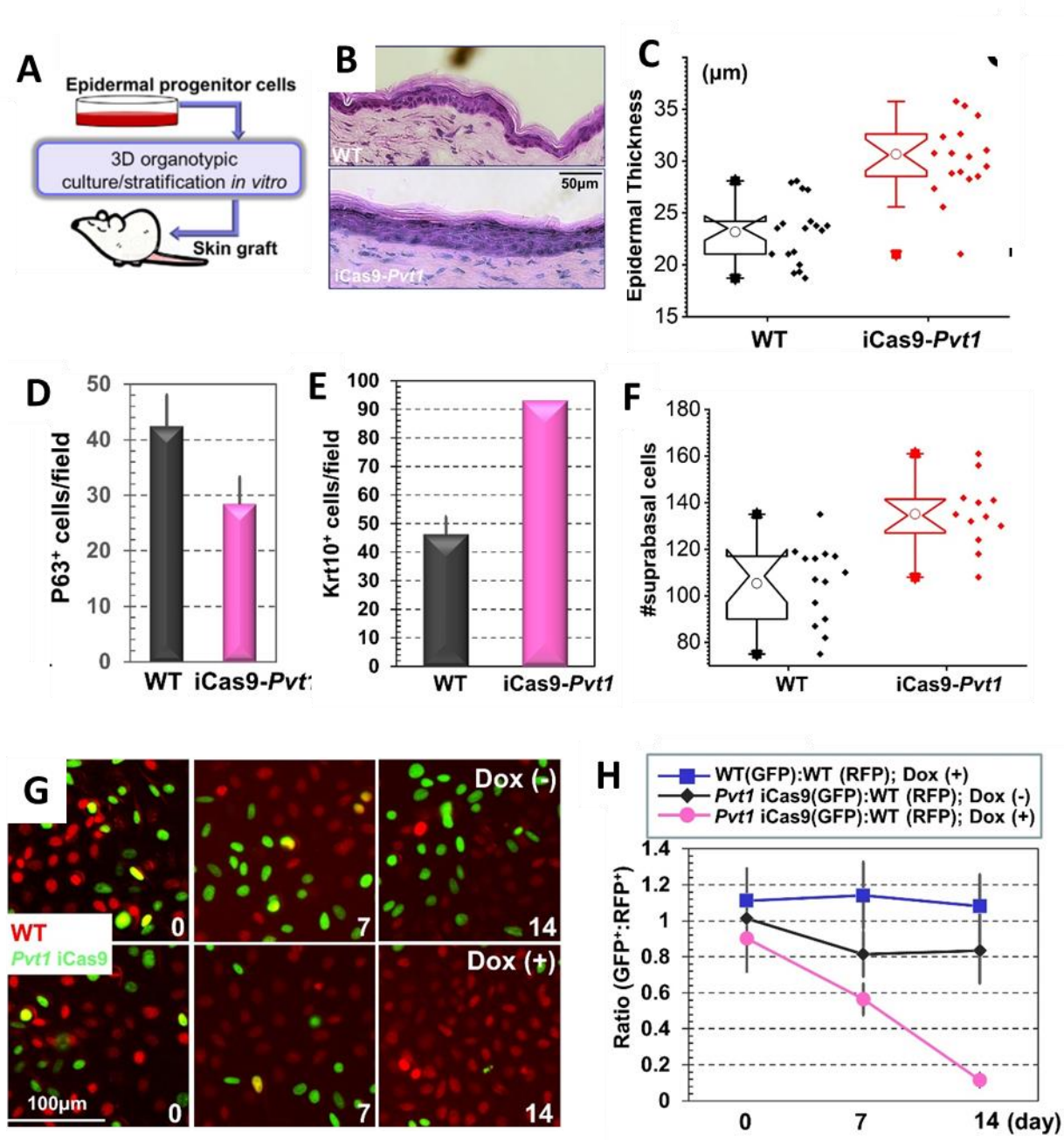

Figure 3.3: Pvt1 regulates epidermal stemness and tissue homeostasis. A. Schematic depicting the process of skin organoid transplant. Epidermal progenitor cells are cultured on top of a dermal matrix isolated from newborn mice to form a 3D organoid, which is subsequently exposed to air to induce differentiation. Finally, the organoid is grafted on the back of a nude mouse. **B.** Skin organoids derived from WT or Pvt1 inducible KO cells were grafted to nude mice. The regenerated skin was analyzed by HE staining. **C.** Epidermal thickness of WT and Pvt1 KO skin grafts was n=18, P<0.01 (Student's t-test). **D.** Number of p63-positive cells in WT and cKO skin was quantified andis shown in a bar graph. n=5, P<0.01 (Student's t-test). Error bar represents SD. **Continued on next page.**

Figure [3.3], continued. E. The number of Krt10 (Keratin 10)-positive epidermal cells in WT or Pvt1 inducible KO skin grafts was quantified andis shown in a bar graph. n=4; P<0.01 (Student's t-test). Error bar represents SD. (standard deviation). **F.** The number of suprabasal epidermal cells in WT or Pvt1 inducible KO skin grafts was quantified andis shown in a box plot. n=14; P<0.01 (Student's t-test). **G.** Fluorescence microscopy demonstrates differing survival capability of WT and Pvt1 inducible KO cells with or without doxycycline (Dox) treatment. **H.** Ratio of WT and Pvt1 inducible KO cells in the co-culture model was quantified andis shown in a dot plot. n=8, P<0.01 (Student's t-test) for KO cells with Dox treatment compared with WT cells or KO cells without Dox stimulation at both Day 7 and 14. Error bar represents SD. The box and whisker plot in **C** and **F** shows the mean (solid diamond within the box), 25th percentile (bottom line of the box), median (middle line of the box), 75th percentile (top line of the box), 5th and 95th percentile (whiskers), 1st and 99th percentile (solid triangles) and minimum and maximum measurements (solid squares).

N^6-methyladenosine modification on Pvt1 enhances its interaction with MYC and protects MYC from rapid degradation

MYC plays a central role in regulating epidermal proliferation and differentiation[17-20]. However, many puzzles still remain regarding how MYC itself is regulated. It is very likely that MYC regulation happens across multiple levels, from the genes to transcripts to protein, simultaneously. It may also be highly dependent on context and cell-type. To confirm the role of MYC in driving epidermal cell proliferation, we performed immunoblotting on differentiated epidermal progenitor cells and found that MYC was decreased at the protein level compared to undifferentiated cells (**Figure 3.4 A**). We next analyzed the RNA-seq data from epidermal cells before and after induced differentiation to probe for evidence of MYC alteration at the transcriptomic level. Gene set enrichment analysis (GSEA) showed that MYC-targeted gene sets are significantly upregulated in epidermal progenitor cells before

differentiation, and they are the gene sets with the highest enrichment scores among the Hallmark (H) gene sets[125] (**Figure 3.4 B**). Using a complementary approach, we also found that MYC-regulated genes are significantly upregulated in epidermal progenitor cells using hierarchical cluster analysis[159] (**Figure 3.4 C**). Interestingly, MYC transcript level per se was not significantly altered when comparing differentiated and undifferentiated epidermal stem cells in our RNA-seq data, suggesting that MYC regulation occurs at a post-transcriptional level.

As a critical signaling molecule, the MYC protein has a relatively short half-life, and its degradation is mediated by phosphorylation at a key threonine residue at its N terminus. Pvt1 interaction with MYC has been shown to inhibit this phosphorylation and protect MYC from protein degradation machinery in cancer cells[154]. Based on our finding that Pvt1 regulates epidermal stem cell through m^6A-modification, we thus speculated that methylation of Pvt1 may act as an "m^6A switch" that regulates its interaction with MYC in this context.

First, we confirmed the interaction between Pvt1 and MYC by immunoprecipitation of the Pvt1-MYC complex and determining the level of Pvt1 transcripts via RT-PCR. As expected, Pvt1 transcripts were greatly enriched after immunoprecipitation compared to input (**Figure 3.4 D**). Next, to show that m^6A modification is required for Pvt1-MYC interaction, we tested Pvt1-MYC interaction using the same RNA-protein immunoprecipitation assay on epidermal progenitor cells before and after induced differentiation. We have previously shown that

differentiated epidermal progenitor cells will have reduced Mettl14 level as well as decreased Pvt1 m^6A level. Consistent with our hypothesis, differentiated epidermal cells showed significant reduction in Pvt1-MYC interaction (**Figure 3.4 E**). However, induced differentiation can result in a wide range of molecular changes in the epidermal cells. It is thus possible that the change in Pvt1-MYC interaction is not directly caused by reduced Pvt1 methylation. To this end, we isolated RNA from epidermal progenitor cells and treated the RNA with FTO, the m^6A eraser protein, to remove the m^6A modification, then tested Pvt1-MYC interaction. FTO treatment has previously been demonstrated as an efficient method to remove m^6A modifications from purified RNA[64]. We were also able to confirm the removal of m^6A on Pvt1 via m^6A pulldown and RT-PCR (**Figure 3.4 F**). We found that after RNA was treated with FTO, Pvt1-MYC interaction is significantly reduced compared to the control group in which the FTO reaction is neutralized by EDTA (**Figure 3.4 G**). We also isolated the RNA from *Pvt1* knockout cells that expressed the Pvt1 mutant with all m^6A modification sites mutated (Pvt1-A5G) and repeated the test. Similarly, the mutant Pvt1-A5G showed significantly less interaction with MYC compared to WT Pvt1 (**Figure 3.4 H**). The results were also the same when we used the Pvt1-A5GT3C mutant, which can restore potential secondary structure disruptions (**Figure 3.4 I**). The concordant results from these complementary Pvt1-MYC interaction assays provide strong evidence that m^6A-modification enhances Pvt1-MYC interaction in epidermal stem cells.

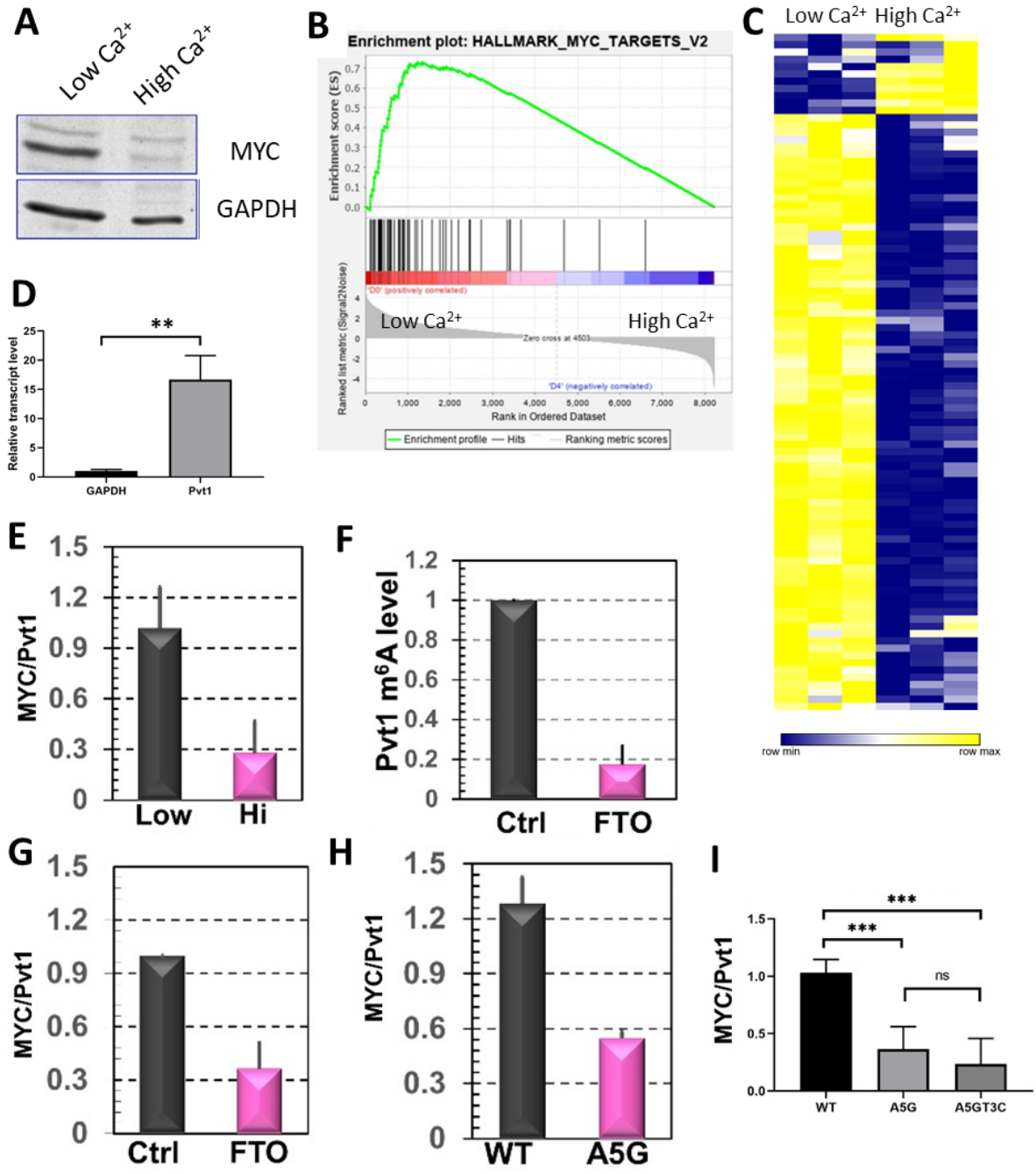

Figure 3.4: Pvt1-MYC interaction is dependent on m^{6}A modification on Pvt1. A. Immunoblots show decreased MYC protein level in keratinocytes after inducing differentiation by calcium shift (high Ca^{2+}). **B.** Gene set enrichment analysis (GSEA) on RNA-seq data. The Hallmark (H) gene sets curated from the Molecular Signatures Database (MSigDB) were analyzed for enrichment significance with 1000 random permutations of gene sets, showing that MYC-targeted gene sets are significantly enriched (nominal-p<0.001, FDR-q<0.25) in epidermal progenitor cells (low Ca^{2+}) compared to after differentiation (high Ca^{2+}). **C.** Unbiased hierarchical cluster analysis (HCA) of MYC-targeted genes using a MYC-upregulated gene set curated by Dang et al. **Continued on next page.**

Figure [3.4], continued. D. Relative transcript level after MYC-RNA immunoprecipitation was determined by RT-PCR using input as a control and quantified using ddC_T method. n=3; P<0.005 (Student's t-test). Error bar represents SD. **E.** Interaction between Pvt1 and MYC was determined by immunoprecipitation followed by RT-PCR. Note the significant decrease in Pvt1 and MYC interaction upon calcium shift-induced differentiation. n=3, P<0.01 (Student's t-test). **F.** Pvt1 m^6A methylation level was determined by α-m^6A immunoprecipitation followed by RT-PCR. Treatment with FTO can significantly reduce Pvt1 methylation. **G.** MYC/Pvt1 interaction significantly decreases after m^6A on Pvt1 was removed by adding FTO. **H.** MYC/Pvt1 interaction is significantly lower in the mutant with m^6A site mutated (A5G) compared to WT Pvt1. **I.** MYC/Pvt1 interaction is also decreased in the Pvt1 A5GT3C mutant that has secondary structure base-pairing restored. Note that the level of decrease is similar between the two mutants A5G and A5GT3C. For D-I, error bars represent SD.

Pvt1-MYC interaction has been shown to increase MYC stability and enhance cell proliferation in cancer cells. However, whether this interaction serves a similar function in epidermal stem cells has not been explored. To this end, we tested MYC stability by evaluating MYC protein levels at different time intervals after addition of cycloheximide, an agent that prevents de novo protein synthesis. We found that MYC protein can remain stable in epidermal progenitor cells for up to three hours (**Figure 3.5 A**). However, when cells are differentiated, MYC was almost completely degraded after one hour (**Figure 3.5 A**). Similarly, epidermal cells with either *Mettl14* or *Pvt1* knocked out showed MYC degradation after one hour (**Figure 3.4 B, C, D**). Taken together, our data suggests that MYC protein can be stabilized by interaction with Pvt1. Importantly, m^6A modification acts as a switch mechanism to trigger Pvt1-MYC interaction.

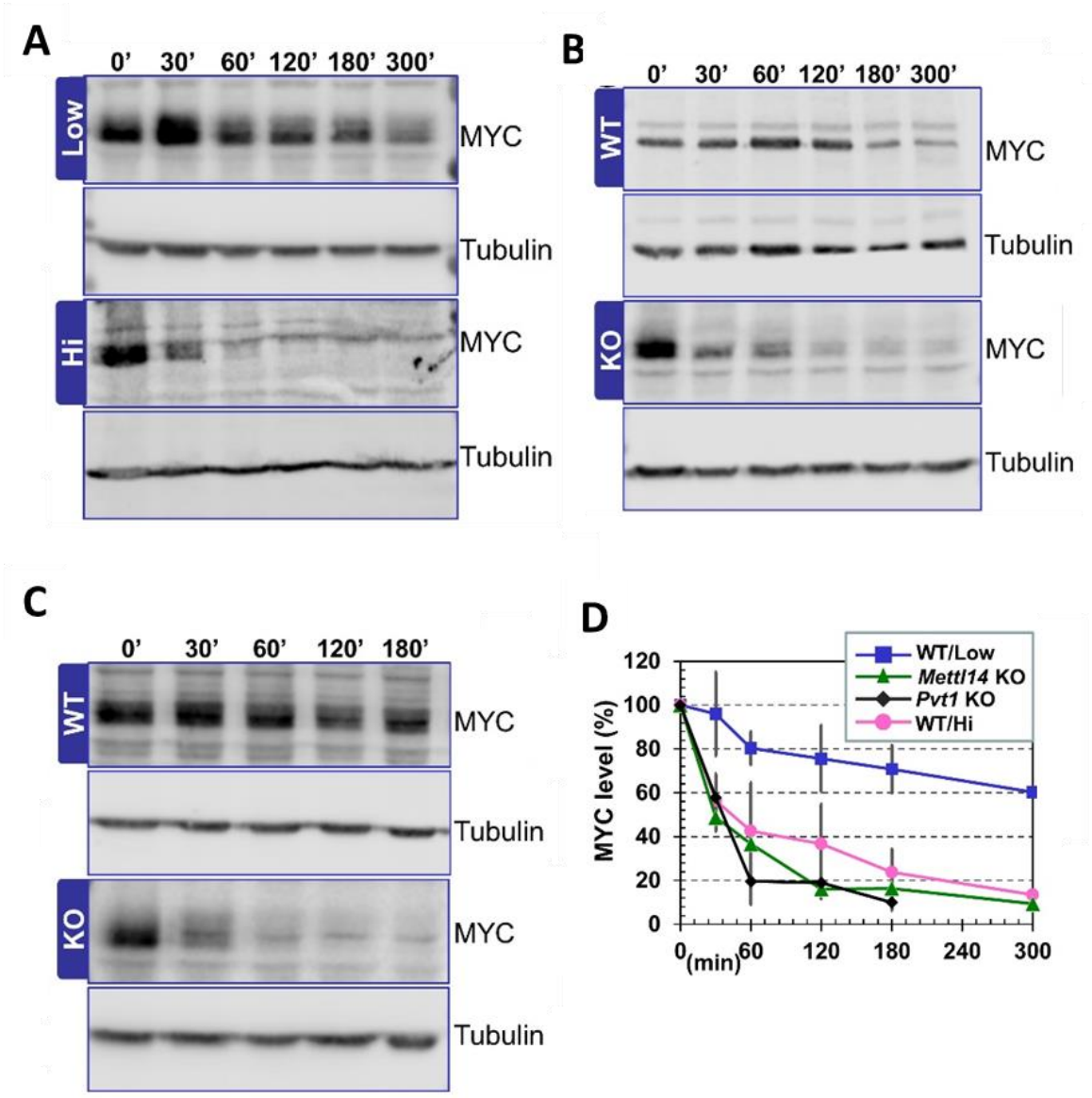

Figure 3.5: **Pvt1-MYC interaction stabilizes MYC. A.** Epidermal progenitor cells before (Low) and after (Hi) calcium shift-induced differentiation were treated with cycloheximide. Cell lysates were collected at 0, 30, 60, 90, 120, 180, and 300 minutes post treatment and subjected to immunoblotting with antibodies against MYC or α-tubulin (internal control). Note the rapid drop in MYC level after induced differentiation. **B-C.** MYC stability was tested on WT versus *Mettl14* cKO (**B**) or WT versus *Pvt1* KO (**C**) epidermal progenitor cells using the same cycloheximide assay. **D.** Band intensity of MYC at different time points after cycloheximide treatment was determined by densitometry and the amount of MYC was calculated and quantified. n=3. Error bar represents SD.

MYC can restore the epidermal stemness defect caused by Mettl14 depletion

We have discovered that loss of *Mettl14* prevents m^6A modification on Pvt1, and without methylation, Pvt1 cannot interact with MYC, resulting in rapid degradation of MYC protein. To confirm the relevance of MYC in this Mettl14-Pvt1-MYC axis in epidermal stemness, we performed a rescue experiment by creating *Mettl14* KO cells with an inducible expression of MYC. In this system, treatment with doxycycline induces MYC expression in a dose-dependent manner (**Figure 3.6 A**).

We prepared skin organoids using the *Mettl14* KO cells with or without inducible MYC and grafted the paired organoids to a host mouse on two sides of its back. We then examined the skin organoids seven days after treating the host with doxycycline. The skin sections revealed a dramatic change between the two organoids on the same host. The *Mettl14* KO organoid resembled the skin from the *Mettl14* KO mice, with increased thickness of the spinous layer and a decreased number of p63-positive basal cells, whereas the *Metll14* KO organoids with inducible MYC resembled skin from WT mice, with normal epidermal thickness and basal cell count (**Figure 3.6 B-F**). This supports our hypothesis that MYC is downstream to the Mettl14-Pvt1 regulation.

We also conducted a MYC rescue experiment using clonal competition assays, as was done previously for *Pvt1* KO cells. As expected, re-expression of MYC enabled the *Mettl14* KO cells to compete with WT cells (**Figure 3.6 G, H**). Taken together, our data indicates that

Mettl14-mediated RNA modification drives epidermal stemness through a Pvt1-MYC signaling cascade.

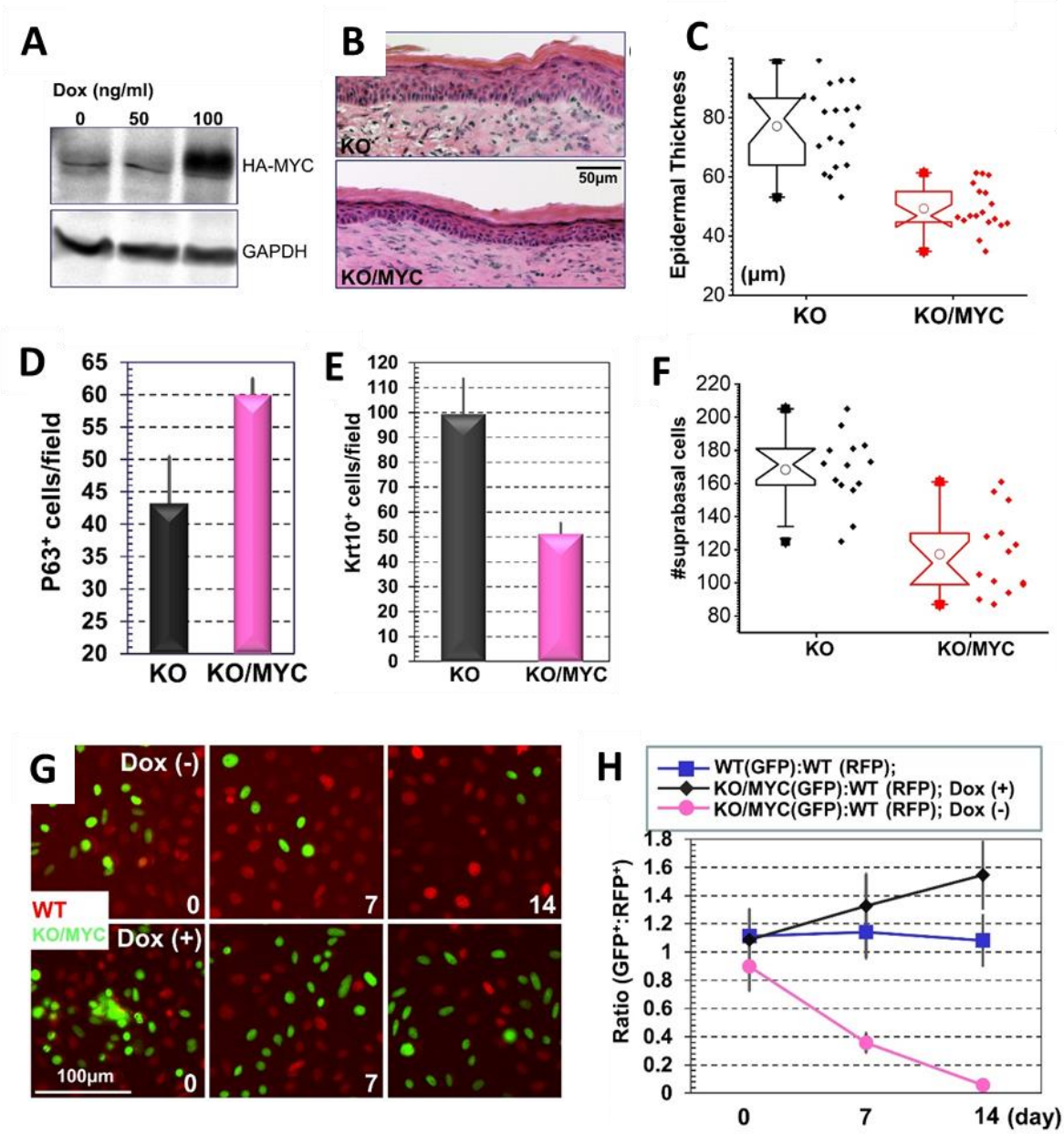

Figure 3.6: MYC can restore skin homeostasis defect in *Mett14* KO skin. A. Immunoblots show inducible expression of MYC upon doxycycline (Dox) stimulation in engineered *Mettl14* KO cells. **B.** Skin organoids derived from *Mettl14* KO cells or KO cells rescued with exogenous expression of MYC were grafted to nude mice. The regenerated skin was analyzed by HE staining. **C.** Epidermal thickness of KO and KO skin rescued with MYC expression was quantified and presented in a box and whisker plot. n=18, P<0.01 (Student's t-test). **Continued on next page.**

Figure [3.6], continued. D. Number of p63-positive cells in KO and KO skin rescued with MYC expression was quantified andis shown in a bar graph. n=5, P<0.01 (Student's t-test). Error bar represents SD. **E.** The number of Krt10 (Keratin 10)-positive epidermal cells in skin grafts derived from *Mettl14* KO cells and KO cells rescued with MYC expression was quantified andis shown in a bar graph. n=4; P<0.01 (Student's t-test). Error bar represents SD. **F.** The number of suprabasal epidermal cells in skin grafts derived from *Mettl14* KO cells and KO cells rescued with MYC expression is shown in a box plot. n=14; P<0.01 (Student's t-test). **G.** Fluorescence microscopy demonstrates different survival capability of WT and *Mettl14* KO cells with inducible expression of MYC. **H.** Ratio of WT and *Mettl14* KO cells with inducible expression of MYC in the co-culture model was quantified and is shown in a dot plot. n=8, P<0.01 (Student's t-test) for KO cells without Dox treatment (no MYC expression) compared with WT cells or KO cells with Dox stimulation (exogenous MYC expression) at both Day 7 and 14. Error bar represents SD.

DISCUSSION

Our results reveal that lncRNA Pvt1 plays a pivotal role in skin tissue homeostasis. Pvt1 associates with MYC protein and prevents its degradation[154], and our data showed that m^6A methylation is an important regulator of this process. Using in vitro culture and skin transplantation models, we showed that RNA m^6A modification mediated by the Mettl3/Mettl14 complex regulates epidermal stemness by controlling Pvt1 and MYC interaction through Pvt1 methylation, uncovering a key and novel molecular mechanism underlying skin tissue homeostasis, regeneration, and wound repair.

MYC is a proto-oncogene critically involved in many cellular processes. In the skin epidermis, deletion of endogenous *MYC* by the *Krt5* promoter-driven expression of *Cre* leads to skin hypoplasia, impaired epidermal stem cell self-renewal, and delayed wound healing in vivo[20], resembling the phenotypes o*f Mettl14* deletion and CRISPR-mediated KO of Pvt1 in

skin epidermal cells. In another study, when *MYC* is ablated by an inducible *Cre-ER* system, tissue homeostasis in adult skin interfollicular epidermis and hair follicles seems to be normal, but cKO skin is more resistant to Ras-induced carcinogenesis as a result of upregulation of p21[160]. Interestingly, constitutive or inducible overexpression of *MYC* in basal progenitor cells causes both increased keratinocyte proliferation and differentiation in vivo. Constitutive *MYC* overexpression driven by the *Krt5* promoter also leads to spontaneous skin carcinogenesis as the animals age[21]. Together, this suggests that MYC plays a multifaceted role in skin tissue homeostasis and tumorigenesis, depending on the level and duration of MYC activation. MYC protein level is significantly reduced in *Mettl14* null cells, and ectopic expression of *MYC* in *Mettl14* KO cells can restore epidermal stemness, strongly suggesting that MYC is a key downstream effector of Mettl14 in regulation of skin tissue homeostasis.

Aberrant skin tissue homeostasis can contribute to the etiology of many skin diseases, including inflammatory skin disorders and skin cancers. Cutaneous SCC (squamous cell carcinoma) is one of the most common cancers in the United States[161,162], and it can be highly invasive and metastatic, leading to severe morbidity and mortality for the patients[163]. Increasing evidence suggests that m^6A modification of mRNA and lncRNA are involved in cancer development and progression[34,112]. Key players in the m^6A pathway, including writer, eraser, and reader proteins, have been shown to play diverse roles in different types of tumorigenesis. Recently, Zhou et al (2019) have shown that expression of METTL3 is upregulated in

cutaneous SCCs and that a knockdown of METTL3 in SCC cell lines in vitro can inhibit tumorigenicity by reducing p63 expression[164]. Understanding the molecular mechanisms underlying epidermal stemness and homeostasis provides an essential basis for developing effective therapies for skin diseases, including skin SCC.

In closing, our studies provide important insights into the molecular mechanisms whereby RNA post-transcriptional modification regulates epidermal stemness and tissue homeostasis.

CHAPTER IV

DISCUSSION AND CONCLUSION

Skin homeostasis and wound repair is driven by the epidermal stem cells located at the basal layer of the skin epidermis, which not only proliferate to replenish the stem cell pool, but also migrate upwards and differentiate to replace the functional upper layers that are continually lost. The delicate balance between cell proliferation, differentiation and death is essential for the function of the skin. Conversely, aberrant tissue homeostasis can lead to dire consequences for our survival. On one end of the spectrum, non-healing skin tissue, as seen commonly in patients with diabetes, can lead to severe infections that can be fatal to patients. On the other end, uncontrolled skin growth can lead to skin tumors such as cutaneous squamous cell carcinoma, one of the most common cancers in the US. Although cutaneous squamous cell carcinoma rarely metastasizes and has a low mortality rate, it is characterized by its highly recurrent nature, resulting in numerous co-morbidities and creating a large psychological and economic burden for patients.

Despite decades of research, there are still many unsolved questions regarding skin homeostasis, in particular about the mechanisms by which the epidermal stem cells regulate transition between cell fates. This lack of understanding has prevented us from developing better treatments for skin conditions at either end of the disease spectrum. For example, treatment for non-healing diabetic skin wounds is usually restricted to passively applying hydrogels, or using skin grafts in severe cases. The condition will ultimately recur, as the

treatment does not target the core of the problem, which lies in the altered state of the epidermal stem cells. Similarly, surgical excision remains the standard of treatment for cutaneous squamous cell carcinoma patients, and no effective medical treatment has been developed to date. There is thus an unmet need to better characterize skin stem cell biology, and to potentially use the findings to develop better treatment options for patients with related skin conditions.

RNA m^6A modification has previously been found essential for the development of embryonic stem cells, as well as other cell types such as neurons. Our study is the first to reveal that RNA m^6A modification is also critical for regulating epidermal stem cells. However, the mechanism in which m^6A modification regulates stem cell fate is vastly different in epidermal stem cells as opposed to embryonic stem cells and neurons. In embryonic stem cells, m^6A modification is integrated into the transcription process of cell fate-related genes. The modified transcripts interact with the reader protein YTHDF2, facilitating the degradation of the transcripts[68]. This allows for rapid turnover of groups of transcripts and is crucial for cell fate transition. In neuronal stem cells, m^6A modification on transcripts of histone-modification genes causes rapid degradation to change the cellular epigenetic landscape[88]. In contrast, while our study points toward Pvt1 as the main m^6A modification target responsible for maintaining epidermal stemness, we did not find a correlation between the level of m^6A modification and transcript level of *Pvt1*, suggesting that m^6A does not determine transcript turnover of Pvt1. Notably, this observation contrasts with that reported in osteosarcoma cells, in which Pvt1

methylation leads to clearance via the YTHDF2 reader protein[153]. This discrepancy likely represents another example of context-dependent regulation in the human body, especially considering that skin and bone lineages separate very early during embryonic development (ectoderm versus mesoderm). Instead, our findings revealed an alternative lncRNA regulatory mechanism, termed "m^{6}A switch", by which the m^{6}A modification changes the properties of an RNA to interact with an RNA-binding protein, in this case, Pvt1-MYC interaction. As has been shown in cancer cells, we were able to further confirm that Pvt1-MYC interaction stabilizes MYC and the transcription of MYC-regulated genes enables epidermal stem cells to maintain stemness.

In conclusion, our research has uncovered a novel mechanism of skin stem cell regulation. The m^{6}A writer proteins Mettl3/Mettl14 methylate lncRNA Pvt1 on two clusters, enhancing Pvt1-MYC interaction and leading to increased MYC stability and transcription of downstream genes that can maintain epidermal stem cell fate (**Figure 4.1**). We believe this represents a paradigm shift in our understanding of epidermal regulation, as previous research has mainly focused on regulation at the genetic and epigenetic level, whereas the level of RNA modification, or "epitranscriptomic" level, has been widely ignored. Importantly, understanding this mechanism will provide us novel drug targets that can potentially improve the lives of patients with skin diseases caused by loss of skin homeostasis.

As with most scientific breakthroughs, our findings also reveal new questions that need to be addressed. While it is impossible to list all of the areas to be subsequently explored, we will summarize some of the more interesting questions in the following sections.

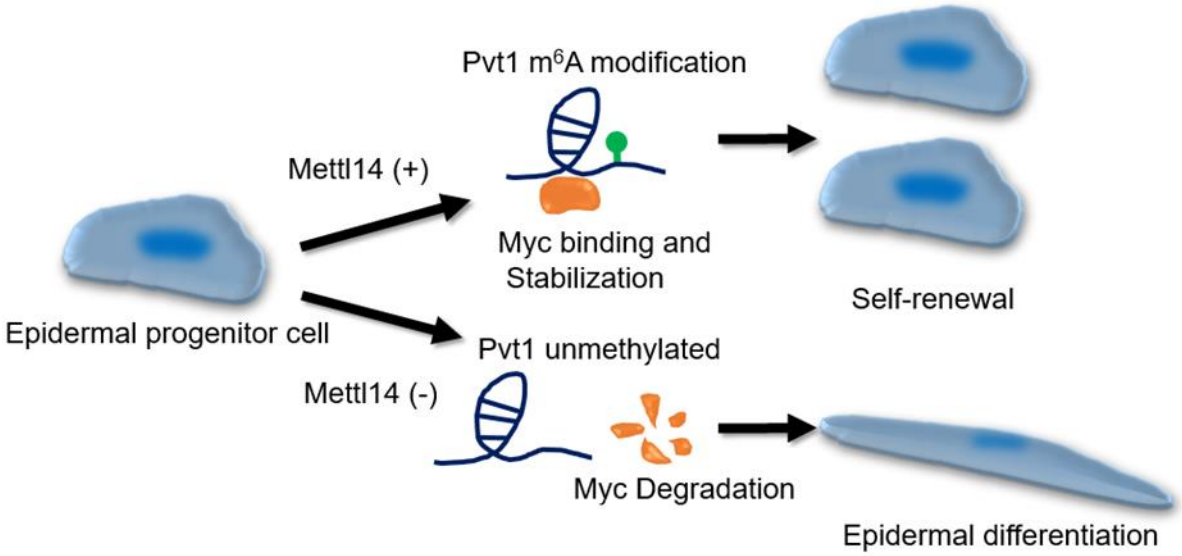

Figure 4.1: Summary of the Mett14-Pvt1-MYC axis in epidermal regulation. In the presence of METTL14, PVT1 is m^6A-modifed, allowing it to bind to MYC and stabilize the protein. MYC can then activate programs that drive stem cell self-renewal. In contrast, loss of METTL14 leads to a decrease in m^6A modification on PVT1. Without the m^6A switch, PVT1 has low affinity to MYC, leading to rapid degradation of MYC and cell differentiation.

FUTURE DIRECTIONS

Do other lncRNAs play a role in epidermal stem cell regulation?

In addition to Pvt1, we found four other lncRNAs (Gas5, Malat1, Neat1, Snhg18) with significant change in methylation level in epidermal progenitor cells after induced differentiation. We focused on Pvt1 first, mainly because it the only lncRNA that has decreased methylation level after differentiation, which is consistent with the drop in Mettl14 expression

in differentiated epidermal cells. However, methylation level can be regulated not only via m^6A writer proteins, but also through eraser proteins. In particular, both FTO and ALKBH5 have been reported to regulate m^6A level in different contexts. It is thus conceivable that the methylation change on the other four lncRNAs may also serve a biological role during epidermal differentiation. To this end, clarifying the potential roles of these lncRNAs will greatly expand our understanding of skin homeostasis.

Gas5 belongs to the *Gas* multigene family, which consists of the genes *Gas1-Gas5*. *Gas* family genes share a common N-terminus but differ in the C-terminus[165]. Gas5 lncRNA has been reported to play a tumor suppressive function in multiple cancers, including lung cancer[166], gastric cancer[167], and liver cancer[168]. Gas5 can interact with various proteins and miRNAs, serving as a molecular sponge or transporter depending on the context, and has been shown to participate in a wide range of signaling pathways, including the DNA damage response pathway, glucocorticoid response pathway, and mTOR/Akt pathway. Studies in gastric cancer cells found that Gas5 can be methylated and YTHDF3 interacts with m^6A-Gas5 to facilitate its degradation[169]. This could be a potential regulatory mechanism in skin epidermis, as our sequencing data showed that after differentiation, there is a significant increase in Gas5 m^6A modification, but a decrease in Gas5 transcript level. Interestingly, Gas5 has also been reported to regulate MYC translation through its interaction with eIF4E[170], and could thus also serve as an additional mechanism to fine-tine MYC level in epidermal stem cells.

Neat1 and Malat1 (also known as Neat2) are lncRNAs with genes located in adjacent regions on the genome, and both genes are highly conserved across vertebrates[171]. The two lncRNAs are also closely related in terms of their localization and functions. Many genetic loci and transcription factors are co-enriched by both Neat1 and Malat1. Neat1 is located in paraspeckles, whereas Malat1 is located in nuclear speckles, and the two may have complementary binding and functions in genome organization[172]. Additionally, both lncRNAs have been reported to be regulated by m^6A-modification, albeit with distinct mechanisms and also under different contexts. In gastric cancer cells, Neat1 may regulate the polycomb repressive complex protein EZH2 via ALKB5-mediated demethylation[173], promoting cell invasion. In esophageal cancer cells, Malat1 with m^6A modification interacts with the m^6A reader YTHDC1 to maintain nuclear speckle organization, which can promote cancer metastasis[174]. Additionally, Malat1 is also the first discovered example of an "m^6A-switch", as m^6A-modification induces a structural change in the Malat1 hairpin and exposes the U_5-tract for recognition and binding to the HNRNPC protein[175]. The interaction between Malat1 and HNRNPC has been reported to play a role in cell cycle regulation in HeLa cells[176], and it would be interesting to see if Malat1-HNRNPC also acts in epidermal stem cell regulation.

Snhg18 is the last lncRNA we found with a change in methylation level during epidermal stem cell differentiation. *Snhg18* belongs to the small nucleolar host gene family of lncRNAs. Many lncRNAs from the *snhg* family have been implicated as playing a role in cancer. Snhg18

has been associated with oncogenic properties in lung cancer[177] and gliomas[178]. However, little information is known in terms of the regulatory mechanism of snhg18.

Our research on Pvt1 will provide us with a framework to tackle the other lncRNAs as well. We can first perform classical knockout or overexpression studies on epidermal progenitor cells in combination with our organoid transplant platform. This will give us an initial impression of the roles these lncRNAs may play in epidermal stem cell regulation. We can next follow the reported evidence from other tissue systems to probe the downstream target of each lncRNA. For example, we can examine whether m^6A-modified Gas5 is degraded by YTHDF3 by knocking down YTHDF3 and determining whether the Gas5 level is increased using RT-PCR. Similarly, for Malat1, we can look for changes in interaction between Malat1 and HNRNPC by RNA-protein immunoprecipitation as we did for Pvt1-MYC. However, as many lncRNAs act in a tissue or cell-type dependent manner, it is possible that we will not find these lncRNA interactions in skin cells. Instead, we may have to resort to large-scale screening studies, such as a CRISPR-Cas9 screening, to look for potential lncRNA targets.

Does circular Pvt1 play any role in the Pvt1-MYC axis in epidermal stem cells?

Circular RNAs (circRNAs) represent a distinctive group of non-coding RNAs (lncRNAs) with a characteristic closed-loop structure. Many linear RNAs also have circular isoforms that are generated through a non-canonical back-splicing mechanism. CircRNAs can regulate cell

function by acting as a sponge against miRNAs or RNA-binding proteins, or interact with proteins as an enhancer or scaffold[179]. In epidermal stem cells, circRNAs have been found to be upregulated during differentiation, though the precise mechanism by which circRNAs regulate epidermal differentiation has not yet been defined[180].

As with mRNAs and lncRNAs, N^6-methyladenosine modification can also be added to circRNAs via the METTL3/METTL14 methyltransferase complex and removed by the eraser protein FTO[181]. Similarly, m^6A modification on circRNAs could also result in different outcomes depending on the reader protein. The reader protein YTHDF2 facilitates the degradation of m^6A-modified circRNA[182], whereas another reader in the same family, YTFDF3, can recruit the protein-initiation complex and translate the m^6A-modified circRNA through a cap-independent process[181]. Interestingly, m^6A-modification can also alter the interaction between circRNA and RNA-binding proteins. For example, m^6A- circNSUN2 interacts with the IGF2BP2 protein to form a complex with HMGA2 mRNA and promote its translation[183].

Based on our finding that m^6A modification on Pvt1 may play a critical role in maintaining epidermal stemness, one potential area to explore is whether the regulatory effect is achieved via Pvt1 or circPvt1; in particular, whether m^6A modification occurs on circPvt1 and whether it can also affect its interaction with MYC. Indeed, circPvt1 has been implicated as playing a role in immune diseases and multiple cancers[184,185], including skin squamous cell carcinoma[186]. Twenty-six circPvt1 isoforms have been documented in the NIH database, CircInteractome

(https://circinteractome.nia.nih.gov/). Curiously, the most common isoform is composed of the entirety of exon 2, which is also where we found the two m^{6}A clusters in our study. One limitation on many previous studies of Pvt1 is the use of conventional RT-PCR, RNA microarray, or RNA-seq methods to study these lncRNAs. These methods cannot reliably detect circRNAs because circRNAs share the same sequence as their linear counterparts. In addition, circRNAs lack the poly-A tail of linear RNAs and thus are usually removed during the RNA isolation process in most RNA-seq protocols.

To determine whether circPvt1 is affected by m^{6}A modification, we can perform RNA m^{6}A immunoprecipitation and RT-PCR to examine the level of m^{6}A-modified Pvt1 compared to circPvt1. To detect circPvt1 with RT-PCR methods, we can use convergent primers that cover the unique back-splicing junction of the circPvt1 isoform to specifically detect circPvt1 and not the linear form. As an additional validation, we can also treat the RNA with RNase R, which specifically degrades linear RNAs but not circRNAs[187]. We can also confirm the m^{6}A modification site by comparing the m^{6}A level of circPvt1 in WT Pvt1 versus the Pvt1-A5G mutant, which lacks the m^{6}A sites. We can determine if MYC protein interacts with m^{6}A-modified Pvt1 by performing MYC RNA-immunoprecipitation and RT-PCR using circPVT1-specific primers (i.e., convergent primers). Finally, to determine if m^{6}A-modified circPVT1 also plays a role in epidermal development, we can knock down circPvt1 by using siRNA

targeting the specific back-splicing junction sites of circPvt1 in epidermal progenitor cells and observe the effect on stemness.

Is m^{6}A-Pvt1-MYC dysregulated in cutaneous squamous cell carcinoma?

Based on the cell of origin, skin cancer can be generally divided into melanocytic (melanoma) or keratinocytic (basal cell carcinoma and squamous cell carcinoma). Clinically and pharmaceutically, melanoma has received broad attention due to its high mortality rate, and as a result, the past decade has seen great advances in understanding the pathobiology of melanoma, leading to major breakthroughs in targeted therapies and immunotherapies. In contrast, non-melanoma skin cancers (NMSC), even though they are the most common malignancy in the US and are associated with significant life and economic burdens, have received little attention in the cancer field[188-190]. Currently, treatment of cutaneous squamous cell carcinoma is largely based on surgical excision. While effective in most cases, the tumor tends to recur locally, which greatly impacts the patients' quality of life and increases their economic burden. In addition, surgical excision is not applicable for patients with advanced or metastatic tumors. There are only two targeted agents approved for cutaneous squamous cell carcinoma, cetuximab and vemodeglib; however, the effectiveness of these drugs is still in question[191,192]. Identifying whether m^{6}A-Pvt1 plays a role in NMSC will be of great interest because it can provide novel drug targets.

There is accumulating evidence that MYC is a driver of cutaneous squamous cell carcinoma. The gene is commonly amplified in squamous cell carcinoma samples[193], and epidermis lacking *MYC* is resistant to Ras-driven tumorigenesis in mouse models[160]. Finally, mice with epidermal expression of the *MYC-T58A* mutant show accelerated skin tumor development in the DMBA/TPA carcinogenesis model[194]. This is of particular interest to us because Pvt1 also stabilizes MYC through phosphorylation of the T58 residue[154]. *METTL3* has recently been found to be upregulated in cutaneous squamous cell carcinoma samples, and *METTL3* knockdown can inhibit tumor growth in vitro and in vivo[164]. Based on our discovery of how m^{6}A-Pvt1 regulates MYC and drives epidermal stemness, it is very plausible that *METTL3/METTL14* is upregulated in cutaneous squamous cell carcinomas, which increases the m^{6}A level of Pvt1, leading to enhanced Pvt1-MYC interaction and stabilization of MYC oncoprotein.

To prove this hypothesis, we can first examine the level of m^{6}A modification in cutaneous squamous cell carcinoma cell lines or tissue samples from patients. We can next evaluate whether our epidermal *Mettl14* cKO mouse is resistant to DMBA/TPA-induced carcinogenesis. Finally, we can graft skin cells with inducible *Pvt1* or the *Pvt1-A5G* mutant that prevents its methylation, and examine whether the tumor-resistance can be removed by external Pvt1 (but not Pvt1-A5G). This will provide strong evidence of the causal effect of m^{6}A-Pvt1 in driving cutaneous squamous cell carcinoma.

How can the discovery of the m^{6}A-Pvt1/MYC axis be translated into a clinical setting?

Skin homeostasis is a tightly regulated process, and aberrant regulation can lead to many human diseases. Lack of epidermal stem cell proliferation and mobility can lead to poor healing of skin wounds, whereas uncontrolled proliferation can result in cutaneous tumors. There is a severe lack of medical options for either of these diseases, and our findings have a potential to fill this niche. Importantly, recent research has reported that RNA m^{6}A-modification is a druggable target, either via an FTO inhibitor[195] or a METTL3 inhibitor[196]. Interestingly, both of these m^{6}A-modifying drugs have been used to successfully treat AML in pre-clinical models, yet these drugs are expected to act in opposing ways in regards to m^{6}A level. FTO inhibition leads to increased methylation, whereas METTL3 inhibition reduces methylation. This observation highlights the context-dependent nature of RNA m^{6}A modifications, as it can be oncogenic or tumor suppressive depending on its target, and extreme care should be taken to minimize potential off-target effects of the drug. The optimal drug design would thus be a targeted approach in which small molecules can be guided to precise subcellular locations where they are expected to function. For example, based on our discovery in epidermal stem cells, lack of RNA m^{6}A modification on Pvt1 leads to decreased epidermal proliferation and migration. Thus, for patients with poor wound healing, we can design an antisense oligonucleotide (ASO) specifically targeting Pvt1 transcript and tether it to an FTO inhibitor. This will restrict FTO inhibition to only affect proteins in close proximity to Pvt1 and greatly

reduce the probability of FTO removing m^6A from other transcripts. Conversely, as we expect Pvt1 methylation to drive cutaneous squamous cell cancer, we can use Pvt1-ASO tethered to a METTL3 inhibitor, which will reduce the m^6A modifications on Pvt1 and decrease its interaction with MYC, leading to MYC degradation and tumor shrinkage (**Figure 4.2**). In summary, understanding the role of m^6A regulation in epidermis has given us potential drug targets that may be utilized to treat various skin diseases caused by homeostasis defects, and using a targeted drug design will allow us to direct small molecular inhibitors to the exact m^6A target to reduce complications caused by off-target drug effects.

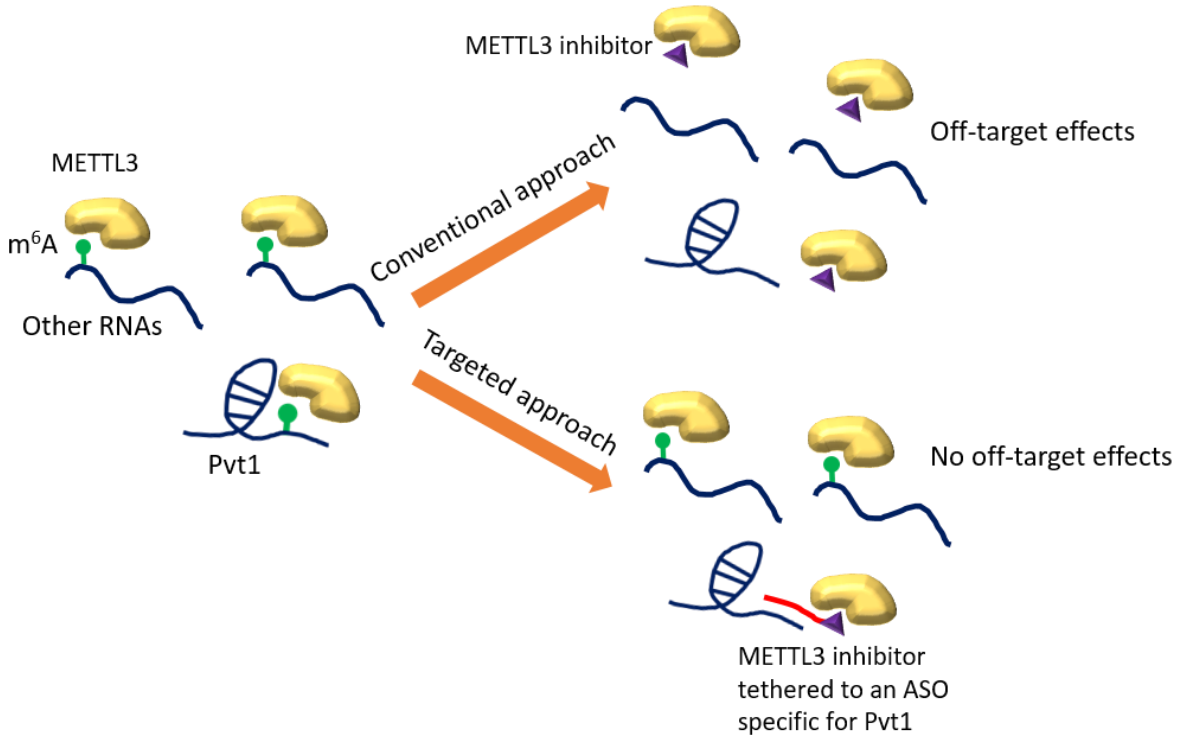

Figure 4.2: Using a targeted approach to design m^{6}A drugs. RNA m^{6}A modification is an important regulatory mechanism for a wide range of mRNAs and lncRNAs (left). Conventional treatment inhibiting METTL3 can reduce the m^{6}A on all RNAs indiscriminately, and cause adverse effects due to removal of m^{6}A from unintentional targets (upper right). By using a targeted approach, such as tethering the METTL3 inhibitor to an antisense oligo (ASO) specific to PVT1, it is possible to greatly reduce off-target effects, as only METTL3 in close proximity to the target (PVT1) will be inhibited (lower right).

REFERENCES

1 Blanpain, C. & Fuchs, E. Epidermal homeostasis: a balancing act of stem cells in the skin. *Nat Rev Mol Cell Biol* **10**, 207-217, doi:10.1038/nrm2636 (2009).

2 Fuchs, E. Scratching the surface of skin development. *Nature* **445**, 834-842, doi:10.1038/nature05659 (2007).

3 Alsaidan, M. *et al.* Hippocrates' Contributions to Dermatology Revealed. *JAMA Dermatol* **151**, 658, doi:10.1001/jamadermatol.2015.0201 (2015).

4 Donati, G. & Watt, F. M. Stem cell heterogeneity and plasticity in epithelia. *Cell Stem Cell* **16**, 465-476, doi:10.1016/j.stem.2015.04.014 (2015).

5 Watt, F. M. Mammalian skin cell biology: at the interface between laboratory and clinic. *Science* **346**, 937-940, doi:10.1126/science.1253734 (2014).

6 Clayton, E. *et al.* A single type of progenitor cell maintains normal epidermis. *Nature* **446**, 185-189, doi:10.1038/nature05574 (2007).

7 Blanpain, C., Horsley, V. & Fuchs, E. Epithelial stem cells: turning over new leaves. *Cell* **128**, 445-458, doi:10.1016/j.cell.2007.01.014 (2007).

8 Alonso, L. & Fuchs, E. Stem cells of the skin epithelium. *Proc Natl Acad Sci U S A* **100 Suppl 1**, 11830-11835, doi:10.1073/pnas.1734203100 (2003).

9 Albert, M. R. & Weinstock, M. A. Keratinocyte carcinoma. *CA Cancer J Clin* **53**, 292-302, doi:10.3322/canjclin.53.5.292 (2003).

10 Fuchs, E. Epithelial Skin Biology: Three Decades of Developmental Biology, a Hundred Questions Answered and a Thousand New Ones to Address. *Current topics in developmental biology* **116**, 357-374, doi:10.1016/bs.ctdb.2015.11.033 (2016).

11 Koster, M. I. p63 in skin development and ectodermal dysplasias. *J Invest Dermatol* **130**, 2352-2358, doi:10.1038/jid.2010.119 (2010).

12 Botchkarev, V. A. & Flores, E. R. p53/p63/p73 in the epidermis in health and disease. *Cold Spring Harb Perspect Med* **4**, doi:10.1101/cshperspect.a015248 (2014).

13 Candi, E. *et al.* Differential roles of p63 isoforms in epidermal development: selective genetic complementation in p63 null mice. *Cell Death Differ* **13**, 1037-1047, doi:10.1038/sj.cdd.4401926 (2006).

14 Rinne, T., Brunner, H. G. & van Bokhoven, H. p63-associated disorders. *Cell Cycle* **6**, 262-268, doi:10.4161/cc.6.3.3796 (2007).

15 Yamanaka, S. & Takahashi, K. [Induction of pluripotent stem cells from mouse fibroblast cultures]. *Tanpakushitsu Kakusan Koso* **51**, 2346-2351 (2006).

16 Park, I. H. *et al.* Reprogramming of human somatic cells to pluripotency with defined factors. *Nature* **451**, 141-146, doi:10.1038/nature06534 (2008).

17 Arnold, I. & Watt, F. M. c-Myc activation in transgenic mouse epidermis results in mobilization of stem cells and differentiation of their progeny. *Curr Biol* **11**, 558-568, doi:10.1016/s0960-9822(01)00154-3 (2001).

18 Waikel, R. L., Kawachi, Y., Waikel, P. A., Wang, X. J. & Roop, D. R. Deregulated expression of c-Myc depletes epidermal stem cells. *Nat Genet* **28**, 165-168, doi:10.1038/88889 (2001).

19 Frye, M., Gardner, C., Li, E. R., Arnold, I. & Watt, F. M. Evidence that Myc activation depletes the epidermal stem cell compartment by modulating adhesive interactions with the local microenvironment. *Development* **130**, 2793-2808, doi:10.1242/dev.00462 (2003).

20 Zanet, J. *et al.* Endogenous Myc controls mammalian epidermal cell size, hyperproliferation, endoreplication and stem cell amplification. *J Cell Sci* **118**, 1693-1704, doi:10.1242/jcs.02298 (2005).

21 Watt, F. M., Frye, M. & Benitah, S. A. MYC in mammalian epidermis: how can an oncogene stimulate differentiation? *Nature reviews. Cancer* **8**, 234-242, doi:10.1038/nrc2328 (2008).

22 Frye, M. & Watt, F. M. The RNA methyltransferase Misu (NSun2) mediates Myc-induced proliferation and is upregulated in tumors. *Curr Biol* **16**, 971-981, doi:10.1016/j.cub.2006.04.027 (2006).

23 Driskell, I. *et al.* The histone methyltransferase Setd8 acts in concert with c-Myc and is required to maintain skin. *EMBO J* **31**, 616-629, doi:10.1038/emboj.2011.421 (2012).

24 Quinn, J. J. & Chang, H. Y. Unique features of long non-coding RNA biogenesis and function. *Nat Rev Genet* **17**, 47-62, doi:10.1038/nrg.2015.10 (2016).

25 Piipponen, M., Nissinen, L. & Kähäri, V. M. Long non-coding RNAs in cutaneous biology and keratinocyte carcinomas. *Cell Mol Life Sci* **77**, 4601-4614, doi:10.1007/s00018-020-03554-3 (2020).

26 Wan, D. C. & Wang, K. C. Long noncoding RNA: significance and potential in skin biology. *Cold Spring Harb Perspect Med* **4**, doi:10.1101/cshperspect.a015404 (2014).

27 Kretz, M. *et al.* Suppression of progenitor differentiation requires the long noncoding RNA ANCR. *Genes Dev* **26**, 338-343, doi:10.1101/gad.182121.111 (2012).

28 Kretz, M. *et al.* Control of somatic tissue differentiation by the long non-coding RNA TINCR. *Nature* **493**, 231-235, doi:10.1038/nature11661 (2013).

29 Lee, C. S. *et al.* Cancer-Associated Long Noncoding RNA SMRT-2 Controls Epidermal Differentiation. *J Invest Dermatol* **138**, 1445-1449, doi:10.1016/j.jid.2018.01.003 (2018).

30 Tanis, S. E. J., Köksal, E. S., van Buggenum, J. A. G. L. & Mulder, K. W. BLNCR is a long non-coding RNA adjacent to integrin beta-1 that is rapidly lost during epidermal progenitor cell differentiation. *Sci Rep* **9**, 31, doi:10.1038/s41598-018-37251-w (2019).

31 Ziegler, C. *et al.* The long non-coding RNA LINC00941 and SPRR5 are novel regulators of human epidermal homeostasis. *EMBO Rep* **20**, doi:10.15252/embr.201846612 (2019).

32 Cai, P. *et al.* A genome-wide long noncoding RNA CRISPRi screen identifies PRANCR as a novel regulator of epidermal homeostasis. *Genome Res* **30**, 22-34, doi:10.1101/gr.251561.119 (2020).

33 Jonkhout, N. *et al.* The RNA modification landscape in human disease. *RNA* **23**, 1754-1769, doi:10.1261/rna.063503.117 (2017).

34 Roundtree, I. A., Evans, M. E., Pan, T. & He, C. Dynamic RNA Modifications in Gene Expression Regulation. *Cell* **169**, 1187-1200, doi:10.1016/j.cell.2017.05.045 (2017).

35 Lavi, U., Fernandez-Muñoz, R. & Darnell, J. E. Content of N-6 methyl adenylic acid in heterogeneous nuclear and messenger RNA of HeLa cells. *Nucleic Acids Res* **4**, 63-69, doi:10.1093/nar/4.1.63 (1977).

36 Dominissini, D. *et al.* The dynamic N(1)-methyladenosine methylome in eukaryotic messenger RNA. *Nature* **530**, 441-446, doi:10.1038/nature16998 (2016).

37 Li, X. *et al.* Transcriptome-wide mapping reveals reversible and dynamic N(1)-methyladenosine methylome. *Nat Chem Biol* **12**, 311-316, doi:10.1038/nchembio.2040 (2016).

38 Schibler, U. & Perry, R. P. The 5'-termini of heterogeneous nuclear RNA: a comparison among molecules of different sizes and ages. *Nucleic Acids Res* **4**, 4133-4149, doi:10.1093/nar/4.12.4133 (1977).

39 Linder, B. *et al.* Single-nucleotide-resolution mapping of m6A and m6Am throughout the transcriptome. *Nat Methods* **12**, 767-772, doi:10.1038/nmeth.3453 (2015).

40 Sendinc, E. *et al.* PCIF1 Catalyzes m6Am mRNA Methylation to Regulate Gene Expression. *Mol Cell* **75**, 620-630.e629, doi:10.1016/j.molcel.2019.05.030 (2019).

41 Desrosiers, R., Friderici, K. & Rottman, F. Identification of methylated nucleosides in messenger RNA from Novikoff hepatoma cells. *Proc Natl Acad Sci U S A* **71**, 3971-3975, doi:10.1073/pnas.71.10.3971 (1974).

42 Dubin, D. T. & Taylor, R. H. The methylation state of poly A-containing messenger RNA from cultured hamster cells. *Nucleic Acids Res* **2**, 1653-1668, doi:10.1093/nar/2.10.1653 (1975).

43 Schaefer, M., Pollex, T., Hanna, K. & Lyko, F. RNA cytosine methylation analysis by bisulfite sequencing. *Nucleic Acids Res* **37**, e12, doi:10.1093/nar/gkn954 (2009).

44 Yang, X. *et al.* 5-methylcytosine promotes mRNA export - NSUN2 as the methyltransferase and ALYREF as an m. *Cell Res* **27**, 606-625, doi:10.1038/cr.2017.55 (2017).

45 Hussain, S. *et al.* NSun2-mediated cytosine-5 methylation of vault noncoding RNA determines its processing into regulatory small RNAs. *Cell Rep* **4**, 255-261, doi:10.1016/j.celrep.2013.06.029 (2013).

46 Khoddami, V. & Cairns, B. R. Identification of direct targets and modified bases of RNA cytosine methyltransferases. *Nat Biotechnol* **31**, 458-464, doi:10.1038/nbt.2566 (2013).

47 Lan, J. *et al.* Functional role of Tet-mediated RNA hydroxymethylcytosine in mouse ES cells and during differentiation. *Nat Commun* **11**, 4956, doi:10.1038/s41467-020-18729-6 (2020).

48 He, C. *et al.* TET2 chemically modifies tRNAs and regulates tRNA fragment levels. *Nat Struct Mol Biol* **28**, 62-70, doi:10.1038/s41594-020-00526-w (2021).

49 Wei, C. M. & Moss, B. Nucleotide sequences at the N6-methyladenosine sites of HeLa cell messenger ribonucleic acid. *Biochemistry* **16**, 1672-1676, doi:10.1021/bi00627a023 (1977).

50 Csepany, T., Lin, A., Baldick, C. J. & Beemon, K. Sequence specificity of mRNA N6-adenosine methyltransferase. *J Biol Chem* **265**, 20117-20122 (1990).

51 Harper, J. E., Miceli, S. M., Roberts, R. J. & Manley, J. L. Sequence specificity of the human mRNA N6-adenosine methylase in vitro. *Nucleic Acids Res* **18**, 5735-5741, doi:10.1093/nar/18.19.5735 (1990).

52 Bokar, J. A., Rath-Shambaugh, M. E., Ludwiczak, R., Narayan, P. & Rottman, F. Characterization and partial purification of mRNA N6-adenosine methyltransferase from HeLa cell nuclei. Internal mRNA methylation requires a multisubunit complex. *J Biol Chem* **269**, 17697-17704 (1994).

53 Liu, J. *et al.* A METTL3-METTL14 complex mediates mammalian nuclear RNA N6-adenosine methylation. *Nat Chem Biol* **10**, 93-95, doi:10.1038/nchembio.1432 (2014).

54 Wang, P., Doxtader, K. A. & Nam, Y. Structural Basis for Cooperative Function of and Mettl14 Methyltransferases. *Mol Cell* **63**, 306-317, doi:10.1016/j.molcel.2016.05.041 (2016).

55 Wang, X. *et al.* Structural basis of N(6)-adenosine methylation by the METTL3-METTL14 complex. *Nature* **534**, 575-578, doi:10.1038/nature18298 (2016).

56 Yu, D. *et al.* Human MettL3-MettL14 RNA adenine methyltransferase complex is active on double-stranded DNA containing lesions. *Nucleic Acids Res*, doi:10.1093/nar/gkab460 (2021).

57 Bertero, A. *et al.* The SMAD2/3 interactome reveals that TGFβ controls m6A mRNA methylation in pluripotency. *Nature* **555**, 256-259, doi:10.1038/nature25784 (2018).

58 Huang, H. *et al.* Histone H3 trimethylation at lysine 36 guides m6A RNA modification co-transcriptionally. *Nature* **567**, 414-419, doi:10.1038/s41586-019-1016-7 (2019).

59 Pendleton, K. E. *et al.* The U6 snRNA m6A Methyltransferase METTL16 Regulates SAM Synthetase Intron Retention. *Cell* **169**, 824-835.e814, doi:10.1016/j.cell.2017.05.003 (2017).

60 Doxtader, K. A. *et al.* Structural Basis for Regulation of METTL16, an S-Adenosylmethionine Homeostasis Factor. *Mol Cell* **71**, 1001-1011.e1004, doi:10.1016/j.molcel.2018.07.025 (2018).

61 Mendel, M. *et al.* Methylation of Structured RNA by the m6A Writer METTL16 Is Essential for Mouse Embryonic Development. *Mol Cell* **71**, 986-1000.e1011, doi:10.1016/j.molcel.2018.08.004 (2018).

62 Ma, H. *et al.* N6-Methyladenosine methyltransferase ZCCHC4 mediates ribosomal RNA methylation. *Nat Chem Biol* **15**, 88-94, doi:10.1038/s41589-018-0184-3 (2019).

63 Ren, W. *et al.* Structure and regulation of ZCCHC4 in m6A-methylation of 28S rRNA. *Nat Commun* **10**, 5042, doi:10.1038/s41467-019-12923-x (2019).

64 Wei, J. *et al.* Differential m6A, m6Am, and m1A Demethylation Mediated by FTO in

the Cell Nucleus and Cytoplasm. *Molecular cell* **71**, 973-985.e975, doi:10.1016/j.molcel.2018.08.011 (2018).

65 Mauer, J. *et al.* Reversible methylation of m6Am in the 5' cap controls mRNA stability. *Nature* **541**, 371-375, doi:10.1038/nature21022 (2017).

66 Zheng, G. *et al.* ALKBH5 is a mammalian RNA demethylase that impacts RNA metabolism and mouse fertility. *Mol Cell* **49**, 18-29, doi:10.1016/j.molcel.2012.10.015 (2013).

67 McTaggart, J. S. *et al.* FTO is expressed in neurones throughout the brain and its expression is unaltered by fasting. *PLoS One* **6**, e27968, doi:10.1371/journal.pone.0027968 (2011).

68 Wang, X. *et al.* N6-methyladenosine-dependent regulation of messenger RNA stability. *Nature* **505**, 117-120, doi:10.1038/nature12730 (2014).

69 Du, H. *et al.* YTHDF2 destabilizes m(6)A-containing RNA through direct recruitment of the CCR4-NOT deadenylase complex. *Nat Commun* **7**, 12626, doi:10.1038/ncomms12626 (2016).

70 Wang, X. *et al.* N(6)-methyladenosine Modulates Messenger RNA Translation Efficiency. *Cell* **161**, 1388-1399, doi:10.1016/j.cell.2015.05.014 (2015).

71 Shi, H. *et al.* m6 A facilitates hippocampus-dependent learning and memory through YTHDF1. *Nature* **563**, 249-253, doi:10.1038/s41586-018-0666-1 (2018).

72 Roundtree, I. A. & He, C. Nuclear m(6)A Reader YTHDC1 Regulates mRNA Splicing. *Trends Genet* **32**, 320-321, doi:10.1016/j.tig.2016.03.006 (2016).

73 Xiao, W. *et al.* Nuclear m(6)A Reader YTHDC1 Regulates mRNA Splicing. *Mol Cell* **61**, 507-519, doi:10.1016/j.molcel.2016.01.012 (2016).

74 Hsu, P. J. *et al.* Ythdc2 is an N 6-methyladenosine binding protein that regulates mammalian spermatogenesis. *Cell Res* **27**, 1115-1127, doi:10.1038/cr.2017.99 (2017).

75 Mao, Y. *et al.* m6A in mRNA coding regions promotes translation via the RNA helicase-containing YTHDC2. *Nat Commun* **10**, 5332, doi:10.1038/s41467-019-

13317-9 (2019).

76 Liu, N. *et al.* N(6)-methyladenosine-dependent RNA structural switches regulate RNA-protein interactions. *Nature* **518**, 560-564, doi:10.1038/nature14234 (2015).

77 Huang, H. *et al.* Recognition of RNA N6-methyladenosine by IGF2BP proteins enhances mRNA stability and translation. *Nat Cell Biol* **20**, 285-295, doi:10.1038/s41556-018-0045-z (2018).

78 Zhu, S. *et al.* An oncopeptide regulates m6A recognition by the m 6 A reader IGF2BP1 and tumorigenesis. *Nat Commun* **11**, 1685, doi:10.1038/s41467-020-15403-9 (2020).

79 Edens, B. M. *et al.* FMRP Modulates Neural Differentiation through m6A-Dependent mRNA Nuclear Export. *Cell Rep* **28**, 845-854.e845, doi:10.1016/j.celrep.2019.06.072 (2019).

80 Wu, R. *et al.* A novel m6A reader Prrc2a controls oligodendroglial specification and myelination. *Cell Res* **29**, 23-41, doi:10.1038/s41422-018-0113-8 (2019).

81 Agarwala, S. D., Blitzblau, H. G., Hochwagen, A. & Fink, G. R. RNA methylation by the MIS complex regulates a cell fate decision in yeast. *PLoS Genet* **8**, e1002732, doi:10.1371/journal.pgen.1002732 (2012).

82 Hongay, C. F. & Orr-Weaver, T. L. Drosophila Inducer of MEiosis 4 (IME4) is required for Notch signaling during oogenesis. *Proc Natl Acad Sci U S A* **108**, 14855-14860, doi:10.1073/pnas.1111577108 (2011).

83 Batista, P. J. *et al.* m(6)A RNA modification controls cell fate transition in mammalian embryonic stem cells. *Cell Stem Cell* **15**, 707-719, doi:10.1016/j.stem.2014.09.019 (2014).

84 Geula, S. *et al.* Stem cells. m6A mRNA methylation facilitates resolution of naive pluripotency toward differentiation. *Science (New York, N.Y.)* **347**, 1002-1006, doi:10.1126/science.1261417 (2015).

85 Frye, M., Harada, B. T., Behm, M. & He, C. RNA modifications modulate gene expression during development. *Science* **361**, 1346-1349,

doi:10.1126/science.aau1646 (2018).

86 Lin, Z. *et al.* Mettl3-/Mettl14-mediated mRNA N6-methyladenosine modulates murine spermatogenesis. *Cell Res* **27**, 1216-1230, doi:10.1038/cr.2017.117 (2017).

87 Yoon, K. J. *et al.* Temporal Control of Mammalian Cortical Neurogenesis by m6A Methylation. *Cell* **171**, 877-889.e817, doi:10.1016/j.cell.2017.09.003 (2017).

88 Wang, Y. *et al.* N6-methyladenosine RNA modification regulates embryonic neural stem cell self-renewal through histone modifications. *Nat Neurosci* **21**, 195-206, doi:10.1038/s41593-017-0057-1 (2018).

89 Wang, C. X. *et al.* METTL3-mediated m6A modification is required for cerebellar development. *PLoS Biol* **16**, e2004880, doi:10.1371/journal.pbio.2004880 (2018).

90 De Jesus, D. F. *et al.* m6A mRNA Methylation Regulates Human β-Cell Biology in Physiological States and in Type 2 Diabetes. *Nat Metab* **1**, 765-774, doi:10.1038/s42255-019-0089-9 (2019).

91 Li, H. B. *et al.* m6A mRNA methylation controls T cell homeostasis by targeting the IL-7/STAT5/SOCS pathways. *Nature* **548**, 338-342, doi:10.1038/nature23450 (2017).

92 Winkler, R. *et al.* m6A modification controls the innate immune response to infection by targeting type I interferons. *Nat Immunol* **20**, 173-182, doi:10.1038/s41590-018-0275-z (2019).

93 Dorn, L. E. *et al.* The N6-Methyladenosine mRNA Methylase METTL3 Controls Cardiac Homeostasis and Hypertrophy. *Circulation* **139**, 533-545, doi:10.1161/CIRCULATIONAHA.118.036146 (2019).

94 Yang, Y. *et al.* Glucose Is Involved in the Dynamic Regulation of m6A in Patients With Type 2 Diabetes. *J Clin Endocrinol Metab* **104**, 665-673, doi:10.1210/jc.2018-00619 (2019).

95 Qin, Y. *et al.* Role of m6A RNA methylation in cardiovascular disease (Review). *Int J Mol Med* **46**, 1958-1972, doi:10.3892/ijmm.2020.4746 (2020).

96 Huang, X., Lv, D., Yang, X., Li, M. & Zhang, H. m6A RNA methylation regulators

could contribute to the occurrence of chronic obstructive pulmonary disease. *J Cell Mol Med* **24**, 12706-12715, doi:10.1111/jcmm.15848 (2020).

97 Han, M. *et al.* Abnormality of m6A mRNA Methylation Is Involved in Alzheimer's Disease. *Front Neurosci* **14**, 98, doi:10.3389/fnins.2020.00098 (2020).

98 Gokhale, N. S. & Horner, S. M. RNA modifications go viral. *PLoS Pathog* **13**, e1006188, doi:10.1371/journal.ppat.1006188 (2017).

99 Vu, L. P. *et al.* The N6-methyladenosine (m 6 A)-forming enzyme METTL3 controls myeloid differentiation of normal hematopoietic and leukemia cells. *Nat Med* **23**, 1369-1376, doi:10.1038/nm.4416 (2017).

100 Weng, H. *et al.* METTL14 Inhibits Hematopoietic Stem/Progenitor Differentiation and Promotes Leukemogenesis via mRNA m. *Cell Stem Cell* **22**, 191-205.e199, doi:10.1016/j.stem.2017.11.016 (2018).

101 Li, Z. *et al.* FTO Plays an Oncogenic Role in Acute Myeloid Leukemia as a N6-Methyladenosine RNA Demethylase. *Cancer Cell* **31**, 127-141, doi:10.1016/j.ccell.2016.11.017 (2017).

102 Li, F. *et al.* N6-Methyladenosine Modulates Nonsense-Mediated mRNA Decay in Human Glioblastoma. *Cancer Res* **79**, 5785-5798, doi:10.1158/0008-5472.CAN-18-2868 (2019).

103 Dong, Z. & Cui, H. The Emerging Roles of RNA Modifications in Glioblastoma. *Cancers (Basel)* **12**, doi:10.3390/cancers12030736 (2020).

104 Cui, Q. *et al.* m6A RNA Methylation Regulates the Self-Renewal and Tumorigenesis of Glioblastoma Stem Cells. *Cell Rep* **18**, 2622-2634, doi:10.1016/j.celrep.2017.02.059 (2017).

105 Li, F. *et al.* m6A RNA Methylation Regulators Participate in the Malignant Progression and Have Clinical Prognostic Value in Lung Adenocarcinoma. *Front Genet* **11**, 994, doi:10.3389/fgene.2020.00994 (2020).

106 Xu, R. *et al.* The momentous role of N6-methyladenosine in lung cancer. *J Cell Physiol* **236**, 3244-3256, doi:10.1002/jcp.30136 (2021).

107 Chang, G. *et al.* YTHDF3 Induces the Translation of m6A-Enriched Gene Transcripts to Promote Breast Cancer Brain Metastasis. *Cancer Cell* **38**, 857-871.e857, doi:10.1016/j.ccell.2020.10.004 (2020).

108 Niu, Y. *et al.* RNA N6-methyladenosine demethylase FTO promotes breast tumor progression through inhibiting BNIP3. *Mol Cancer* **18**, 46, doi:10.1186/s12943-019-1004-4 (2019).

109 Chen, M. *et al.* RNA N6-methyladenosine methyltransferase-like 3 promotes liver cancer progression through YTHDF2-dependent posttranscriptional silencing of SOCS2. *Hepatology* **67**, 2254-2270, doi:10.1002/hep.29683 (2018).

110 Chen, Y. *et al.* WTAP facilitates progression of hepatocellular carcinoma via m6A-HuR-dependent epigenetic silencing of ETS1. *Mol Cancer* **18**, 127, doi:10.1186/s12943-019-1053-8 (2019).

111 He, L. *et al.* Functions of N6-methyladenosine and its role in cancer. *Mol Cancer* **18**, 176, doi:10.1186/s12943-019-1109-9 (2019).

112 Deng, X. *et al.* RNA N6-methyladenosine modification in cancers: current status and perspectives. *Cell Res* **28**, 507-517, doi:10.1038/s41422-018-0034-6 (2018).

113 Ezhkova, E. *et al.* Ezh2 orchestrates gene expression for the stepwise differentiation of tissue-specific stem cells. *Cell* **136**, 1122-1135, doi:10.1016/j.cell.2008.12.043 (2009).

114 Dauber, K. L. *et al.* Dissecting the Roles of Polycomb Repressive Complex 2 Subunits in the Control of Skin Development. *J Invest Dermatol* **136**, 1647-1655, doi:10.1016/j.jid.2016.02.809 (2016).

115 Avgustinova, A. & Benitah, S. A. Epigenetic control of adult stem cell function. *Nat Rev Mol Cell Biol* **17**, 643-658, doi:10.1038/nrm.2016.76 (2016).

116 Wu, X., Kodama, A. & Fuchs, E. ACF7 regulates cytoskeletal-focal adhesion dynamics and migration and has ATPase activity. *Cell* **135**, 137-148, doi:10.1016/j.cell.2008.07.045 (2008).

117 Wu, X., Suetsugu, S., Cooper, L. A., Takenawa, T. & Guan, J. L. Focal adhesion kinase regulation of N-WASP subcellular localization and function. *J Biol Chem* **279**, 9565-9576, doi:10.1074/jbc.M310739200 (2004).

118 Dominissini, D. *et al.* Topology of the human and mouse m6A RNA methylomes revealed by m6A-seq. *Nature* **485**, 201-206, doi:10.1038/nature11112 (2012).

119 Meng, J. *et al.* A protocol for RNA methylation differential analysis with MeRIP-Seq data and exomePeak R/Bioconductor package. *Methods* **69**, 274-281, doi:10.1016/j.ymeth.2014.06.008 (2014).

120 Kim, D., Langmead, B. & Salzberg, S. L. HISAT: a fast spliced aligner with low memory requirements. *Nat Methods* **12**, 357-360, doi:10.1038/nmeth.3317 (2015).

121 Liu, L., Zhang, S. W., Huang, Y. & Meng, J. QNB: differential RNA methylation analysis for count-based small-sample sequencing data with a quad-negative binomial model. *BMC Bioinformatics* **18**, 387, doi:10.1186/s12859-017-1808-4 (2017).

122 Love, M. I., Huber, W. & Anders, S. Moderated estimation of fold change and dispersion for RNA-seq data with DESeq2. *Genome Biol* **15**, 550, doi:10.1186/s13059-014-0550-8 (2014).

123 Maere, S., Heymans, K. & Kuiper, M. BiNGO: a Cytoscape plugin to assess overrepresentation of gene ontology categories in biological networks. *Bioinformatics* **21**, 3448-3449, doi:10.1093/bioinformatics/bti551 (2005).

124 Mootha, V. K. *et al.* PGC-1alpha-responsive genes involved in oxidative phosphorylation are coordinately downregulated in human diabetes. *Nat Genet* **34**, 267-273, doi:10.1038/ng1180 (2003).

125 Subramanian, A. *et al.* Gene set enrichment analysis: a knowledge-based approach for interpreting genome-wide expression profiles. *Proc Natl Acad Sci U S A* **102**, 15545-15550, doi:10.1073/pnas.0506580102 (2005).

126 Meng, T. G. *et al.* Mettl14 is required for mouse postimplantation development by facilitating epiblast maturation. *FASEB J* **33**, 1179-1187, doi:10.1096/fj.201800719R (2019).

127 Vasioukhin, V., Degenstein, L., Wise, B. & Fuchs, E. The magical touch: genome targeting in epidermal stem cells induced by tamoxifen application to mouse skin. *Proc Natl Acad Sci U S A* **96**, 8551-8556, doi:10.1073/pnas.96.15.8551 (1999).

128 Lavker, R. M. & Sun, T. T. Heterogeneity in epidermal basal keratinocytes: morphological and functional correlations. *Science* **215**, 1239-1241, doi:10.1126/science.7058342 (1982).

129 Loeffler, M., Potten, C. S. & Wichmann, H. E. Epidermal cell proliferation. II. A comprehensive mathematical model of cell proliferation and migration in the basal layer predicts some unusual properties of epidermal stem cells. *Virchows Arch B Cell Pathol Incl Mol Pathol* **53**, 286-300 (1987).

130 Potten, C. S., Wichmann, H. E., Loeffler, M., Dobek, K. & Major, D. Evidence for discrete cell kinetic subpopulations in mouse epidermis based on mathematical analysis. *Cell Tissue Kinet* **15**, 305-329, doi:10.1111/j.1365-2184.1982.tb01050.x (1982).

131 Potten, C. S. & Loeffler, M. Epidermal cell proliferation. I. Changes with time in the proportion of isolated, paired and clustered labelled cells in sheets of murine epidermis. *Virchows Arch B Cell Pathol Incl Mol Pathol* **53**, 279-285 (1987).

132 Morris, R. J., Fischer, S. M. & Slaga, T. J. Evidence that the centrally and peripherally located cells in the murine epidermal proliferative unit are two distinct cell populations. *J Invest Dermatol* **84**, 277-281, doi:10.1111/1523-1747.ep12265358 (1985).

133 Mascré, G. *et al.* Distinct contribution of stem and progenitor cells to epidermal maintenance. *Nature* **489**, 257-262, doi:10.1038/nature11393 (2012).

134 Rompolas, P. *et al.* Spatiotemporal coordination of stem cell commitment during epidermal homeostasis. *Science* **352**, 1471-1474, doi:10.1126/science.aaf7012 (2016).

135 Sada, A. *et al.* Defining the cellular lineage hierarchy in the interfollicular epidermis of adult skin. *Nat Cell Biol* **18**, 619-631, doi:10.1038/ncb3359 (2016).

136 Mesa, K. R. *et al.* Homeostatic Epidermal Stem Cell Self-Renewal Is Driven by Local Differentiation. *Cell Stem Cell* **23**, 677-686.e674, doi:10.1016/j.stem.2018.09.005

(2018).

137 Dekoninck, S. & Blanpain, C. Stem cell dynamics, migration and plasticity during wound healing. *Nat Cell Biol* **21**, 18-24, doi:10.1038/s41556-018-0237-6 (2019).

138 Jones, P. H., Harper, S. & Watt, F. M. Stem cell patterning and fate in human epidermis. *Cell* **80**, 83-93, doi:10.1016/0092-8674(95)90453-0 (1995).

139 Green, H., Rheinwald, J. G. & Sun, T. T. Properties of an epithelial cell type in culture: the epidermal keratinocyte and its dependence on products of the fibroblast. *Prog Clin Biol Res* **17**, 493-500 (1977).

140 Rheinwald, J. G. & Green, H. Serial cultivation of strains of human epidermal keratinocytes: the formation of keratinizing colonies from single cells. *Cell* **6**, 331-343, doi:10.1016/s0092-8674(75)80001-8 (1975).

141 Blanpain, C. & Fuchs, E. Epidermal stem cells of the skin. *Annu Rev Cell Dev Biol* **22**, 339-373, doi:10.1146/annurev.cellbio.22.010305.104357 (2006).

142 Liu, J. *et al.* m6 A mRNA methylation regulates AKT activity to promote the proliferation and tumorigenicity of endometrial cancer. *Nat Cell Biol* **20**, 1074-1083, doi:10.1038/s41556-018-0174-4 (2018).

143 Siegle, J. M. *et al.* SOX2 is a cancer-specific regulator of tumour initiating potential in cutaneous squamous cell carcinoma. *Nat Commun* **5**, 4511, doi:10.1038/ncomms5511 (2014).

144 Yue, J. P., Gou, X. W., Li, Y. Y., Wicksteed, B. & Wu, X. Y. Engineered Epidermal Progenitor Cells Can Correct Diet-Induced Obesity and Diabetes. *Cell Stem Cell* **21**, 256-+, doi:10.1016/j.stem.2017.06.016 (2017).

145 Li, Y. *et al.* Genome-edited skin epidermal stem cells protect mice from cocaine-seeking behaviour and cocaine overdose. *Nat Biomed Eng* **3**, 105-113, doi:10.1038/s41551-018-0293-z (2019).

146 Yuspa, S. H., Kilkenny, A. E., Steinert, P. M. & Roop, D. R. Expression of murine epidermal differentiation markers is tightly regulated by restricted extracellular calcium concentrations in vitro. *The Journal of cell biology* **109**, 1207-1217,

doi:10.1083/jcb.109.3.1207 (1989).

147 Meyer, K. D. & Jaffrey, S. R. Rethinking m6 A Readers, Writers, and Erasers. *Annu Rev Cell Dev Biol* **33**, 319-342, doi:10.1146/annurev-cellbio-100616-060758 (2017).

148 Hardy, M. H. The secret life of the hair follicle. *Trends Genet* **8**, 55-61, doi:10.1016/0168-9525(92)90350-d (1992).

149 Millar, S. E. Molecular mechanisms regulating hair follicle development. *J Invest Dermatol* **118**, 216-225, doi:10.1046/j.0022-202x.2001.01670.x (2002).

150 Berardesca, E. & Maibach, H. I. Transepidermal water loss and skin surface hydration in the non invasive assessment of stratum corneum function. *Derm Beruf Umwelt* **38**, 50-53 (1990).

151 Indra, A. K. & Leid, M. Epidermal permeability barrier measurement in mammalian skin. *Methods Mol Biol* **763**, 73-81, doi:10.1007/978-1-61779-191-8_4 (2011).

152 Panatta, E. *et al.* Long non-coding RNA uc.291 controls epithelial differentiation by interfering with the ACTL6A/BAF complex. *EMBO Rep* **21**, e46734, doi:10.15252/embr.201846734 (2020).

153 Chen, S., Zhou, L. & Wang, Y. ALKBH5-mediated m6A demethylation of lncRNA PVT1 plays an oncogenic role in osteosarcoma. *Cancer Cell Int* **20**, 34, doi:10.1186/s12935-020-1105-6 (2020).

154 Tseng, Y.-Y. *et al.* PVT1 dependence in cancer with MYC copy-number increase. *Nature* **512**, 82-86, doi:10.1038/nature13311 (2014).

155 Cao, J. *et al.* An easy and efficient inducible CRISPR/Cas9 platform with improved specificity for multiple gene targeting. *Nucleic Acids Res* **44**, e149, doi:10.1093/nar/gkw660 (2016).

156 Li, R., Zhuang, Y., Han, M., Xu, T. & Wu, X. piggyBac as a high-capacity transgenesis and gene-therapy vector in human cells and mice. *Dis Model Mech* **6**, 828-833, doi:10.1242/dmm.010827 (2013).

157 Cho, S. W. *et al.* Promoter of lncRNA Gene PVT1 Is a Tumor-Suppressor DNA

Boundary Element. *Cell* **173**, 1398-1412.e1322, doi:10.1016/j.cell.2018.03.068 (2018).

158 Gruber, A. R., Lorenz, R., Bernhart, S. H., Neuböck, R. & Hofacker, I. L. The Vienna RNA websuite. *Nucleic Acids Res* **36**, W70-74, doi:10.1093/nar/gkn188 (2008).

159 Zeller, K. I., Jegga, A. G., Aronow, B. J., O'Donnell, K. A. & Dang, C. V. An integrated database of genes responsive to the Myc oncogenic transcription factor: identification of direct genomic targets. *Genome Biol* **4**, R69, doi:10.1186/gb-2003-4-10-r69 (2003).

160 Oskarsson, T. *et al.* Skin epidermis lacking the c-Myc gene is resistant to Ras-driven tumorigenesis but can reacquire sensitivity upon additional loss of the p21Cip1 gene. *Genes Dev* **20**, 2024-2029, doi:10.1101/gad.381206 (2006).

161 Preston, D. S. & Stern, R. S. Nonmelanoma cancers of the skin. *N Engl J Med* **327**, 1649-1662, doi:10.1056/NEJM199212033272307 (1992).

162 Alam, M. & Ratner, D. Cutaneous squamous-cell carcinoma. *N Engl J Med* **344**, 975-983, doi:10.1056/NEJM200103293441306 (2001).

163 Burton, K. A., Ashack, K. A. & Khachemoune, A. Cutaneous Squamous Cell Carcinoma: A Review of High-Risk and Metastatic Disease. *Am J Clin Dermatol* **17**, 491-508, doi:10.1007/s40257-016-0207-3 (2016).

164 Zhou, R. *et al.* METTL3 mediated m6A modification plays an oncogenic role in cutaneous squamous cell carcinoma by regulating ΔNp63. *Biochem Biophys Res Commun* **515**, 310-317, doi:10.1016/j.bbrc.2019.05.155 (2019).

165 Ragni, E., Fontaine, T., Gissi, C., Latgè, J. P. & Popolo, L. The Gas family of proteins of Saccharomyces cerevisiae: characterization and evolutionary analysis. *Yeast* **24**, 297-308, doi:10.1002/yea.1473 (2007).

166 Shi, X. *et al.* A critical role for the long non-coding RNA GAS5 in proliferation and apoptosis in non-small-cell lung cancer. *Mol Carcinog* **54 Suppl 1**, E1-E12, doi:10.1002/mc.22120 (2015).

167 Dong, X. *et al.* Association between lncRNA GAS5, MEG3, and PCAT-1

Polymorphisms and Cancer Risk: A Meta-Analysis. *Dis Markers* **2020**, 6723487, doi:10.1155/2020/6723487 (2020).

168 Zhao, P., Cui, X., Zhao, L., Liu, L. & Wang, D. Overexpression of Growth-Arrest-Specific Transcript 5 Improved Cisplatin Sensitivity in Hepatocellular Carcinoma Through Sponging miR-222. *DNA Cell Biol* **39**, 724-732, doi:10.1089/dna.2019.5282 (2020).

169 Ni, W. *et al.* Long noncoding RNA GAS5 inhibits progression of colorectal cancer by interacting with and triggering YAP phosphorylation and degradation and is negatively regulated by the m. *Mol Cancer* **18**, 143, doi:10.1186/s12943-019-1079-y (2019).

170 Hu, G., Lou, Z. & Gupta, M. The long non-coding RNA GAS5 cooperates with the eukaryotic translation initiation factor 4E to regulate c-Myc translation. *PLoS One* **9**, e107016, doi:10.1371/journal.pone.0107016 (2014).

171 Hutchinson, J. N. *et al.* A screen for nuclear transcripts identifies two linked noncoding RNAs associated with SC35 splicing domains. *BMC Genomics* **8**, 39, doi:10.1186/1471-2164-8-39 (2007).

172 West, J. A. *et al.* The long noncoding RNAs NEAT1 and MALAT1 bind active chromatin sites. *Mol Cell* **55**, 791-802, doi:10.1016/j.molcel.2014.07.012 (2014).

173 Zhang, J. *et al.* ALKBH5 promotes invasion and metastasis of gastric cancer by decreasing methylation of the lncRNA NEAT1. *J Physiol Biochem* **75**, 379-389, doi:10.1007/s13105-019-00690-8 (2019).

174 Wang, X. *et al.* N6-methyladenosine modification of MALAT1 promotes metastasis via reshaping nuclear speckles. *Dev Cell* **56**, 702-715.e708, doi:10.1016/j.devcel.2021.01.015 (2021).

175 Zhou, K. I. *et al.* N(6)-Methyladenosine Modification in a Long Noncoding RNA Hairpin Predisposes Its Conformation to Protein Binding. *J Mol Biol* **428**, 822-833, doi:10.1016/j.jmb.2015.08.021 (2016).

176 Yang, F., Yi, F., Han, X., Du, Q. & Liang, Z. MALAT-1 interacts with hnRNP C in cell cycle regulation. *FEBS Lett* **587**, 3175-3181, doi:10.1016/j.febslet.2013.07.048

(2013).

177 Fan, H. *et al.* MKL1-induced lncRNA SNHG18 drives the growth and metastasis of non-small cell lung cancer via the miR-211-5p/BRD4 axis. *Cell Death Dis* **12**, 128, doi:10.1038/s41419-021-03399-z (2021).

178 Zheng, R., Yao, Q., Li, X. & Xu, B. Long Noncoding Ribonucleic Acid SNHG18 Promotes Glioma Cell Motility via Disruption of α-Enolase Nucleocytoplasmic Transport. *Front Genet* **10**, 1140, doi:10.3389/fgene.2019.01140 (2019).

179 Kristensen, L. S. *et al.* The biogenesis, biology and characterization of circular RNAs. *Nat Rev Genet* **20**, 675-691, doi:10.1038/s41576-019-0158-7 (2019).

180 Kristensen, L. S., Okholm, T. L. H., Venø, M. T. & Kjems, J. Circular RNAs are abundantly expressed and upregulated during human epidermal stem cell differentiation. *RNA Biol* **15**, 280-291, doi:10.1080/15476286.2017.1409931 (2018).

181 Yang, Y. *et al.* Extensive translation of circular RNAs driven by N6-methyladenosine. *Cell Res* **27**, 626-641, doi:10.1038/cr.2017.31 (2017).

182 Park, O. H. *et al.* Endoribonucleolytic Cleavage of m6 A-Containing RNAs by RNase P/MRP Complex. *Mol Cell* **74**, 494-507.e498, doi:10.1016/j.molcel.2019.02.034 (2019).

183 Chen, R. X. *et al.* N6-methyladenosine modification of circNSUN2 facilitates cytoplasmic export and stabilizes HMGA2 to promote colorectal liver metastasis. *Nat Commun* **10**, 4695, doi:10.1038/s41467-019-12651-2 (2019).

184 Adhikary, J. *et al.* Circular PVT1: an oncogenic non-coding RNA with emerging clinical importance. *J Clin Pathol* **72**, 513-519, doi:10.1136/jclinpath-2019-205891 (2019).

185 Ghetti, M., Vannini, I., Storlazzi, C. T., Martinelli, G. & Simonetti, G. Linear and circular PVT1 in hematological malignancies and immune response: two faces of the same coin. *Mol Cancer* **19**, 69, doi:10.1186/s12943-020-01187-5 (2020).

186 Chen, S. *et al.* RNA-Seq Profiling of Circular RNAs and the Oncogenic Role of circPVT1 in Cutaneous Squamous Cell Carcinoma. *Onco Targets Ther* **13**, 6777-

6788, doi:10.2147/OTT.S252233 (2020).

187 Szabo, L. & Salzman, J. Detecting circular RNAs: bioinformatic and experimental challenges. *Nat Rev Genet* **17**, 679-692, doi:10.1038/nrg.2016.114 (2016).

188 Apalla, Z., Nashan, D., Weller, R. B. & Castellsague, X. Skin Cancer: Epidemiology, Disease Burden, Pathophysiology, Diagnosis, and Therapeutic Approaches. *Dermatology and therapy* **7**, 5-19, doi:10.1007/s13555-016-0165-y (2017).

189 Cakir, B. O., Adamson, P. & Cingi, C. Epidemiology and economic burden of nonmelanoma skin cancer. *Facial plastic surgery clinics of North America* **20**, 419-422, doi:10.1016/j.fsc.2012.07.004 (2012).

190 Lomas, A., Leonardi-Bee, J. & Bath-Hextall, F. A systematic review of worldwide incidence of nonmelanoma skin cancer. *The British journal of dermatology* **166**, 1069-1080, doi:10.1111/j.1365-2133.2012.10830.x (2012).

191 Wollina, U. Update of cetuximab for non-melanoma skin cancer. *Expert opinion on biological therapy* **14**, 271-276, doi:10.1517/14712598.2013.876406 (2014).

192 Jacobsen, A. A., Aldahan, A. S., Hughes, O. B., Shah, V. V. & Strasswimmer, J. Hedgehog Pathway Inhibitor Therapy for Locally Advanced and Metastatic Basal Cell Carcinoma: A Systematic Review and Pooled Analysis of Interventional Studies. *JAMA dermatology* **152**, 816-824, doi:10.1001/jamadermatol.2016.0780 (2016).

193 Toll, A. *et al.* MYC gene numerical aberrations in actinic keratosis and cutaneous squamous cell carcinoma. *The British journal of dermatology* **161**, 1112-1118, doi:10.1111/j.1365-2133.2009.09351.x (2009).

194 Wang, X. *et al.* Altering MYC phosphorylation in the epidermis increases the stem cell population and contributes to the development, progression, and metastasis of squamous cell carcinoma. *Oncogenesis* **9**, 79, doi:10.1038/s41389-020-00261-3 (2020).

195 Huang, Y. *et al.* Small-Molecule Targeting of Oncogenic FTO Demethylase in Acute Myeloid Leukemia. *Cancer Cell* **35**, 677-691.e610, doi:10.1016/j.ccell.2019.03.006 (2019).

196 Yankova, E. *et al.* Small-molecule inhibition of METTL3 as a strategy against myeloid leukaemia. *Nature* **593**, 597-601, doi:10.1038/s41586-021-03536-w (2021).